inflammation with necrosis (n=23, group 2), and diffuse inflammatory infiltrates with multifocal necrosis (classic myocarditis, n=20, group 3). Other potential causes of death included pneumonia, seizure disorder, sarcoidosis, cancer, and heart disease.
Results: The mean age of group 3 (24 ± 18 years) was significantly lower than groups 1 and 2. There was no significant gender difference across groups (total 27F, 40 M). The mean heart weight was lowest (330 grams) in group 3 (p=0.09). The mean extent of infiltrates (p=0.02) and degree of myocyte necrosis (p=0.05) correlated inversely with the presence of other potential causes of death. Eosinophils were present in 21 cases (31%), and were most frequent in group 1, although there 7 group 3 cases with eosinophils (necrotizing eosinophilic myocarditis). Lymphocytes (n=22), macrophages (n=12), and neutrophils (n=12) were the predominant cell types in the other cases, with 9, 3, and 1 case(s) respectively in group 3. There was no significant differences rates of drug exposure and predominant cell type (overall 58%), although lymphocytic myocarditis was most frequently associated with antibiotic use, and neutrophils with neuroleptic drug use.
Conclusions: We conclude that the extent of infiltrates and myocyte necrosis are greatest in sudden death without other potential cause. Diffuse necrotizing eosinophilic myocarditis represented an unexpectedly high proportion of diffuse myocarditis, but was often not associated with a specific drug etiology.

32 Distribution of Lesions in Sudden Unexpected Deaths by Sarcoidosis

Yang Zhang, Allen P Burke. University of Maryland, Baltimore, MD.
Background: Sarcoidosis is a multisystem disease of uncertain etiology that may be responsible for sudden and unexpected death. There are few autopsy series of patterns of multisystem involvement by sarcoidosis. We herein characterize a series of sarcoidosis from a single medical examiner's office to study the distribution of lesions in sarcoidosis and correlate distribution with clinicopathologic parameters.
Design: A retrospective search of sudden sarcoidosis death was performed from a state-wide medical examiner system over 11-year period. Extent of disease and clinical history was correlated with cause of death. There were 29 sudden deaths due to sarcoidosis identified.
Results: Of the 29 cases, 25 deaths were caused by cardiac sarcoidosis with a presumed mechanism of cardiac arrhythmias. There were 4 deaths due to pulmonary sarcoidosis. These 4 cases of pulmonary sarcoidosis presented with massive lung involvement resulting in pulmonary failure, associated pneumonia, meningeal involvement, and the presence of cocaine in the urine. Lung involvement was also grossly present in 20 of 25 cases of sudden cardiac deaths. Of the 29 cases, 21 (72.4%) patients were clinically undiagnosed. A history of sarcoid was elicited in 6/25 (24%) of cardiac deaths and 2/4 (50%) of the pulmonary deaths. In our study, grossly evident sarcoid with histologic granulomas was also present in lymph nodes (n=17), liver (n=11), kidneys (n=7), spleen (6), and brain (n=3). Cardiac distribution involved the left ventricle in 44%, right ventricle in 44%, and epicardium in 40% of the cardiac sarcoidosis cases. At least 3 organs were involved in 66%, and 2 organs in 90% of the cases.
Conclusions: The current study of fatal sarcoidosis shows that in a medical examiner's population, most cases are due to cardiac involvement. Interestingly, most cases also had pulmonary involvement, even though the small group of pulmonary deaths did not show gross cardiac disease. However, in both groups, extensive involvement of other organs was typical. There is a high rate of cardiac involvement in forensic series because of a bias towards unexpected arrhythmic deaths; related to this is a lower rate of prior history of sarcoidosis in cardiac vs. pulmonary deaths.

Bone and Soft Tissue Pathology

33 NTRK1 Associated Gene Fusions in Pediatric Fibroblastic / Myofibroblastic Neoplasms: A Molecular Study of 58 Cases

Narasimhan P Agaram, Lei Zhang, Yun-Shao Sung, Chun-Liang Chen, Catherine Chung, Christopher Fletcher, Cristina Antonescu. Memorial Sloan Kettering Cancer Center, New York, NY; The Hospital for Sick Children, Toronto, ON, Canada; Brigham and Women's Hospital, Boston, MA.
Background: The spectrum of pediatric fibroblastic and myofibroblastic soft tissue tumors includes a number of locally aggressive neoplasms with sometimes overlapping morphology, such as myofibroma/myofibromatosis (MYO), lipofibromatosis (LPF), fibrous hamartoma of infancy (FHI), and calcifying aponeurotic fibroma, among others. As no prior study has carried out a comprehensive genetic investigation in this group of tumors, we applied the latest whole transcriptome sequencing for better molecular classification and to evaluate potential shared pathogenesis.
Design: RNA sequencing and FusionSeq analysis was performed on 9 cases (4 LPF, 1 FHI and 4 MYO) for novel fusion gene discovery. Validated fusion candidates by RT-PCR were then screened using FISH in a large cohort of cases.
Results: 58 cases were selected - 28 LPF, 11 FHI and 19 MYO. RNA sequencing identified gene fusions in 3/9 cases: 2 LPF showed *TPM3-NTRK1* and *EWSR1-SMAD3* fusions and 1 MYO a *TPR-NTRK1* fusion. The 2 *NTRK1*-rearranged cases showed strong expression for NTRK1 by IHC. Further screening by FISH showed another LPF with *TPM3-NTRK1* fusion, while 18 additional LPFs displayed recurrent complex FISH abnormalities at the 1q22-23.1 locus (that includes *NTRK1* and a number of known *NTRK1*-fusion partners in other cancers). Ten of 11 FHI cases showed recurrent abnormalities in the same 1q22-23.1 region. In contrast only 2 additional MYO cases (2/18) showed 1q22-23.1 FISH abnormalities. No additional *EWSR1* gene rearrangements were identified in 7 cases tested.
Conclusions: Our results show recurrent *NTRK1* related gene fusions in a subset of LPF and rare MYO lesions. The high rate of 1q22-23.1 locus FISH alterations spanning the *NTRK1* gene in both LPF and FHI suggests the possibility of recurrent intra-chromosomal fusions / regional abnormalities. These alterations require a higher resolution methodology for more detailed characterization.

34 Primary Adult Skeletal Osteosarcoma: A Clinicopathological and Molecular Study

Deepu Alex, Lu Wang, George Jour, Sumit Middha, Raghu Chandramohan, John Healey, Khedoudja Nafa, Meera Hameed. Memorial Sloan Kettering Cancer Center, New York, NY.
Background: Osteosarcoma is the most common primary skeletal sarcoma with bimodal age distribution occurring in adolescents (10-14 years) and older individuals above 40 years. Compared to pediatric osteosarcoma, it has been reported that adult skeletal osteosarcoma (>19 years) has a worse outcome. Herein, we investigate the clinicopathological and molecular features of a series of primary adult skeletal osteosarcomas and explore potential morphological and molecular parameters that may affect outcome.
Design: 18 cases of primary adult skeletal osteosarcomas were retrieved and reviewed. Clinical history and follow up were obtained through electronic record review. DNA from FFPE tissue was extracted and processed from 8 cases. DNA copy number alterations (CNA) and allelic imbalances (AI) were analyzed by genome-wide high-resolution SNP-array (OncoScan, Affymetrix).
Results: Our series include 18 patients [male=9, female=9] with a median age of 30 years (19-58) and a median follow up of 52 months (2 months - 19 years). Tumor morphologies were variable and included undifferentiated high grade/pleomorphic sarcoma (n=8), osteoblastic (n=5), chondroblastic (n=2), giant cell rich (n=1), telangiectatic (n=1) and sclerotic (n=1) sub types. Tumor sites included axial (n=7) and extremities (n=11). Five patients (28%) died of disease. Nine (50%) showed no evidence of disease while seven (39%) showed local recurrence and/or metastasis at last follow-up. Genomic analysis of oncogenes and tumor suppressor genes implicated in pediatric osteosarcoma showed frequent copy number alterations (gains and losses) in all 8 cases studied. Most common alterations included loss of heterozygosity, including deletion and copy neutral-LOH, of tumor suppressor genes *TP53* (50%), *CDKN2A* (63%), *RB1* (63%), *PTEN* (50%), *NF1* (50%) and *LSAMP* (63%). Homozygous deletion of *CDKN2A* was found in 25% of cases. In addition, amplifications or copy number gains of oncogenes were present as follows: *CDC5L, RUNX2* and *CCND3* at 6p.12-21 in 37% cases, MYC at 8q24 in 50% cases, *MDM2* and *CDK4* at 12q13-15 in 37% cases, *EGFR* in 25% cases.
Conclusions: 1) Our findings suggest that the primary adult skeletal osteosarcomas share many of the genetic alterations seen in pediatric osteosarcomas.
2) Follow-up showed 39% with local recurrence and/or metastatic disease and 28% died of disease.
3) Additional cases are being studied by SNP-array analysis and targeted next generation sequencing which may aid in the detection of genetic alterations that may be specific to primary adult skeletal osteosarcomas and thus may provide insight into their clinical behavior.

35 Histologic Spectrum of Giant Cell Tumor (GCT) of Bone in Patients < 18 Years of Age: A Study of 66 Patients

Alyaa Al-Ibraheemi, Jodi M Carter, Riyam T Zreik, Carrie Y Inwards, Karen Fritchie. Mayo Clinic, Rochester, MN; Scott & White Healthcare, Temple, TX.
Background: While the majority of GCTs occur in adult patients, occasionally they arise in the pediatric population. In this setting they may be mistaken for tumors more commonly seen in this age group, particularly osteosarcoma due to aggressive radiologic findings and the presence of immature bone. In order to better understand how to avoid this problem, we studied a series of GCTs in patients ≤18 years of age with an emphasis on the histologic features.
Design: All cases of primary GCT of bone in patients ≤18 years were retrieved from our institutional archives. H&E slides were examined with focus on: patterns of bone formation and fibrosis, mitotic activity, necrosis, atypia and collections of foamy histiocytes. Clinical records/radiologic data were reviewed in all cases.
Results: 66 (of 710) patients with histologically confirmed GCT of bone ≤ 18 years of age, including 45 females and 21 males (age range 8 to 18 years, median 16.5 years), were identified. Tumors involved the tibia (17), femur (14), sacrum (8), vertebral bodies (7), radius (5), humerus (4), metacarpal bone (3), fibula (2), and 1 each of the phalanyx, ulna, pelvis, patella, calcaneus and navicular bone. Of cases with available imaging, 24 were epiphyseal, 9 were metaphyseal, and 5 involved both. Mature bone was present in 19 tumors (29%); 36 tumors (54%) had irregular lace-like osteoid and 3 cases (4%) exhibited concentric whorls of osteoid. Zones of dense fibrosis, at times mimicking osteoid, were present in 28 of 66 cases (42%). The mitotic rate ranged from 1-35 mitoses/10 HPFs (median 5), necrosis was present in 12 tumors (18%), and 8 (12%) displayed collections of foamy histiocytes. None of the tumors showed cytologic anaplasia. Follow-up information (N=56, 6 to 840 months, median 83 months) showed 19 patients with local recurrence, and 1 with benign GCT lung metastasis. The median mitotic rates for those patients without recurrence, with recurrence and with metastasis were: 5 (range 1-35), 7 (range 1-24) and 7. 50% of tumors with necrosis recurred (6/12) compared to a recurrence rate of 11% (6/54) in tumors lacking necrosis.
Conclusions: GCT arising in the pediatric population is rare, representing 9% of GCTs seen at our institution. The morphologic spectrum of these tumors is broad and similar to that seen in patients >18 years of age. It is important to recognize patterns of osteoid deposition and fibrosis, seen in over 50% of tumors, and the common occurrence of mitotic activity in order to avoid a mistaken diagnosis of osteosarcoma, particularly on limited biopsy specimens.

36 Fibrous Hamartoma of Infancy- A Clinicopathologic Study of 122 Cases, Including 2 with Malignant Progression

Alyaa Al-Ibraheemi, Anthony Martinez, Sharon W Weiss, Harry Kozakewich, Antonio Perez-Atayde, Karen Fritchie, Andrew L Folpe. Mayo Clinic, Rochester, MN; Emory University, Atlanta, GA; Boston Children's Hospital, Boston, MA.

Background: Fibrous hamartoma of infancy (FHI) is a rare soft tissue lesion of infants and young children with characteristic triphasic morphology. FHI typically occurs in the axilla and rarely other locations. Although FHI is currently characterized as a "hamartoma", its morphological features and clinical behavior suggest it may be a neoplasm. Owing to its rarity, the natural history of FHI and its potential for aggressive behavior is not fully defined.

Design: Available slides from 138 cases diagnosed as "FHI" were retrieved from our archives. Sixteen cases were excluded, leaving a final study population of 122 cases. Follow-up was obtained. Selected cases were tested for *PDGFB* or *ETV6* genes rearrangements.

Results: Cases occurred in 92 M and 30 F (mean age- 18 months; range- birth to 14 years) and involved the axilla (n=23), upper arm (n=20), back (n=20), chest (n=10), thigh (n=11), neck (n=10), scrotal/inguinal region (n=9), buttock (n=4), abdomen (n=4), breast (n=3), cheek (n=2), finger (n=2), forearm (n=2), clavicular soft tissue (n=1) and sacral soft tissue (n=1). Four were congenital. The tumors presented as subcutaneous masses and ranged from 0.5-17 cm (mean 3 cm). All displayed triphasic morphology, although the relative percentages of fat, fibroblastic fascicles and primitive mesenchyme varied widely. Hyalinized zones with cracking artifact, mimicking giant cell fibroblastoma (GCFB), were present in a subset of cases; however *PDGFB* FISH was negative in 3 tested cases. In addition to classical FHI, 2 cases contained large sarcomatous foci with high cellularity, high nuclear grade and brisk mitotic activity. One occurred in a 10-month old F as a new mass in a congenital FHI, and the other as a leg mass in a 6-year-old M. *ETV6* rearrangement was negative in the tumor from the 10-month-old F. Follow-up (26 patients; range: 1 month-208 months, median: 20 months) showed only 2 local recurrences and no metastases. Extensive local disease in the 10-month-old F with sarcomatous FHI necessitated forequarter amputation.

Conclusions: The majority of FHI show typical triphasic morphology. A small subset with less obvious triphasic morphology may be mistaken for various adipocytic, fibroblastic and myxoid tumors of childhood. Most notably, sclerotic variants of FHI closely resemble GCFB and may require molecular analysis for *PDGFB* rearrangement. The exceptional presence of sarcoma within FHI supports the view that these are complex mesenchymal tumors rather than "hamartomas."

37 Malignant Tenosynovial Giant Cell Tumor- A Clinicopathological and Immunohistochemical Study of 7 Cases

Alyaa Al-Ibraheemi, Andre Oliveira, Andrew L Folpe. Mayo Clinic, Rochester, MN.

Background: Tenosynovial giant cell tumors (TGCT) are relatively common tumors of tendons/joints that grow in localized and diffuse patterns and are characterized by a distinctive admixture of cell types, including synoviocyte-like cells, macrophages, larger hemosiderin-laden eosinophilic cells and osteoclasts. By immunohistochemistry (IHC), TGCT contain clusterin and desmin-positive cells (likely synoviocytes) and cells expressing histiocytic markers (e.g., CD163, CD68, CD11c). Genetically, TGCT often contain *CSF1* rearrangements, typically partnered with *COL6A3*. Malignant tenosynovial giant cell tumors (MTGCT), consisting of benign TGCT coexisting with sarcoma (primary MTGCT), or representing sarcomatous recurrences of previously diagnosed benign TGCT (secondary MTGCT), are very rare and poorly characterized. We studied a series of MTGCT in order to better understand their natural history and pathogenesis.

Design: All available slides from 9 cases previously coded as "MTGCT" were retrieved from our archives. Only cases that clearly demonstrated a pre-existing benign TGCT were included, leaving a final group of 7 cases. Immunohistochemistry for desmin, clusterin, CD163, CD68, and CD11c was performed. Clinical and follow-up information was obtained.

Results: Cases occurred in 5 M and 2 F (mean age: 55 years; range: 32-72 years), and involved the ankle/foot (n=2), finger/toe (n=2), pelvic region (n=2), and thigh (n=1). There were 5 primary and 2 secondary MTGCT. Benign areas contained clusterin-positive, hemosiderin-laden, eosinophilic cells, scattered desmin-positive dendritic cells, and many CD163/CD68/CD11c-positive small histiocytes. Sarcomatous foci lacked expression of all markers and consisted either of malignant-appearing large, round cells embedded in a hyalinized matrix or pleomorphic spindled cells. Osteocartilaginous matrix was present in 1 case. Mitotic activity was high (mean 18/10 HPF) and necrosis was present in 3 cases. Follow-up (7 patients; range 1 month to 66 months; mean 19 months) showed 3 patients dead of disease, with lung and lymph node metastases in 3 patients.

Conclusions: MTGCT are aggressive sarcomas with significant potential for adverse patient outcome. Our IHC studies suggest these lesions are not derived from the clusterin, desmin, or CD163/CD68/CD11c-positive cell populations present in benign TGCT, or lose expression of these markers as they acquire a malignant phenotype. On-going FISH and RT-PCR studies for *CSF1* rearrangement and the *CSF1-COL6A3* fusion should help to clarify the molecular pathogenesis of MTGCT.

38 A New Simple Low-Cost Multiplexed Targeted Sequencing Assay to Detect Recurrent Fusion Genes in Sarcomas

Emilie Angot, Philippe Ruminy, Vinciane Marchand, France Blanchard, Élodie Colasse, Marie Cornic, Christian Bastard, Fabrice Jardin, Jean-Christophe Sabourin. University Hospital, Rouen, France; Centre Henri Becquerel, Rouen, France.

Background: Sarcomas represent a heterogeneous group of tumors comprising more than 50 histological different types. Ten to fifteen percent of sarcomas are characterized by specific chromosomal translocations which are routinely used as molecular markers for diagnosis, providing crucial information for prognosis and therapeutic decision. Today, translocations are detected by FISH or RT-PCR. However, these methods can only detect a limited number of transcripts simultaneously. Since the development of high throughput sequencing, the number of specific translocations continues to grow and it seems that we have reached the limits of this molecular "one-shot" approach.

Design: We have developed a simple low-cost (less than 6 dollars per patient) assay based on multiplex ligation-dependent RT-PCR for simultaneous screening of more than 50 rearrangements present in sarcomas. To validate this assay, we selected 42 formalin fixed and paraffin embedded (FFPE) sarcomas with known molecular alteration. In the case of non-contributive results, we repeated the analyses with snap-frozen tissue.

Results: We detected fusion transcript for 9 synovial sarcomas (9/9), 9 alveolar rhabdomyosarcomas (9/9), 4 Ewing sarcomas (4/6), 2 Ewing like sarcomas with *BCOR-CCNB3* fusion transcript (2/2), 6 myxoid liposarcomas (6/7), 2 desmoplastic small round cell tumors (2/2), 1 dermatofibrosarcoma protuberans (1/2), 1 clear cell sarcoma (1/1), 2 angiomatoid fibrous histiocytomas (2/2), 1 infantile fibrosarcoma (1/1) and 1 solitary fibrous tumor (1/1). For 7 tumors, sequence quality was only reached using cryopreserved tissue. We did not detect transcript for 2 primary bone Ewing sarcomas and 1 dermatofibrosarcoma protuberans. Unfortunately, for these latter tumors we did not have cryopreserved tissue. One myxoid liposarcoma transcript was not detected using FFPE and cryopreserved tissue.

Conclusions: We have developed a multiplexed assay which can reveal a large number of gene fusions in sarcomas with good sensitivity and excellent specificity. These promising results provide an opening for this new rapid simple low-cost multiplexed targeted sequencing assay as an alternative method to FISH and RT-PCR for routine diagnosis.

39 TERT Promoter Mutations and Prognosis in Solitary Fibrous Tumor

Armita Bahrami, Seungjae Lee, Inga-Marie Schaefer, Jennifer M Boland, Kurt T Patton, Christopher Fletcher. St. Jude Children's Research Hospital, Memphis, TN; Brigham & Women's Hospital, Boston, MA; Mayo Clinic, Rochester, MN; Trumbull Laboratories, Germantown, TN.

Background: Solitary fibrous tumor (SFT) is a mesenchymal neoplasm exhibiting a broad spectrum of biological behaviors. Clinicopathologic parameters are currently used in risk prediction models for SFT, but the molecular determinants of malignancy in SFTs are unknown. We hypothesized that the activation of telomere maintenance pathways confers a perpetual malignant phenotype in these tumors. Therefore, we investigated *TERT* promoter mutations as a potential underlying mechanism for *TERT* expression in SFT.

Design: *TERT* promoter mutational analysis was performed by PCR and Sanger sequencing in samples from 80 patients with SFT of pleural/pulmonary (*n*=31) or soft tissue (*n*=49) origin. Telomerase expression was assessed by using reverse transcription quantitative real-time PCR (RT-qPCR) in pleural SFTs from 26 patients for whom adequate tumor tissue was available. *TERT* promoter mutation and telomerase expression status were correlated with clinicopathologic risk groups and outcomes.

Results: Patients were stratified into clinicopathologically high-risk (*n*=19), moderate-risk (*n*=24), and low-risk (*n*=37) subgroups by using the risk stratification model proposed by Demicco *et al*. Hotspot *TERT* promoter mutations (22 C228T; 2 C250T) were identified in 24 (30%) patients with SFT: -13 high-risk, 10 moderate-risk, and 1 low-risk patients. RT-qPCR revealed that the presence of *TERT* promoter mutations correlated with high *TERT* expression levels (Figure 1).

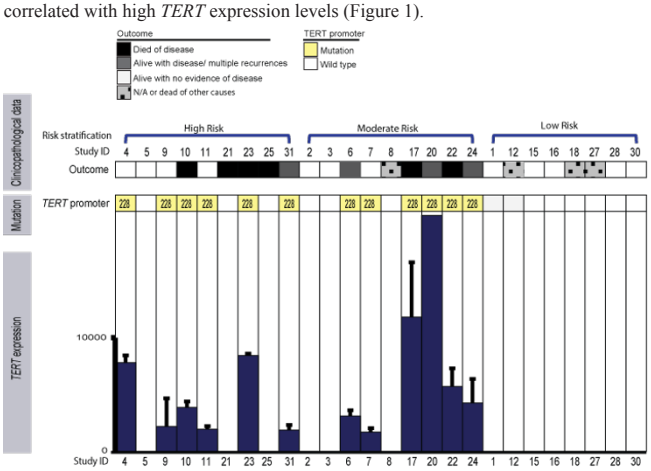

Figure 1. The association of TERT promoter mutations and TERT expression by RT-qPCR with outcome in 26 patients with pleural solitary fibrous tumor

Outcome data were available so far for 39 patients. In 11 of 15 (73%) patients with a mutant *TERT* promoter, the SFT behaved aggressively (recurrent disease/death), whereas only 3 of 24 (13%) patients with the wild-type *TERT* promoter SFT had poor outcomes.

Conclusions: Our data suggest that *TERT* promoter mutations are the molecular mechanism underlying *TERT* expression in a majority of malignant SFTs. Adding *TERT* promoter mutations as a molecular marker to the existing multivariable risk prediction model is expected to improve risk prediction in patients with SFT. The molecular events governing the maintenance of telomeres in the subset of malignant SFTs having the wild-type *TERT* promoter remain to be determined.

40 Analysis of GNAS Mutations in a Series of Intramuscular Myxomas with Identification of a Novel R201L Mutation

Ryan Berry, JIn Wu, Therese Bocklage. University of New Mexico, Albuquerque, NM.

Background: GNAS mutations have been implicated in the development of tumors associated with McCune Albright Syndrome (MAS, endocrine tumors and fibrous dysplasia [FD]) and in Mazabraud's syndrome (FD and intramuscular myxomas [IM]). Further, GNAS mutations have been identified in non-syndromic cases of IM (57%) and FD (72%, range 23-100%). Codon 201 exon 8 of GNAS is the most frequently involved with R201H (53% in IM and 66% in FD) and R201C (44% in IM and 31% in FD) being the most common. Other mutations involving codon 201 have been reported in FD and in patients with MAS, but not in IM.

Design: Twenty-two cases of IM were confirmed by H&E and radiographic imaging. Three cases were excluded due to insufficient material. Four cases of juxta-articular myxoma (JA) were used as negative controls. PCR and direct sequencing were used to analyze codon 201 exon 8 GNAS mutation status using genomic DNA isolated from FFPE samples.

Results: GNAS mutations were identified in 10/19 (53%) cases of IM, with R201C (argine to cysteine) in 8 (80%), R201H (arginine to histidine) in 1 (10%), and a novel R201L (arginine to leucine) in 1 (10%) of the mutated cases. No mutations were detected in the 4 cases of JA.

	# of cases	# WT GNAS (%)	# R201C (% of mutated)	# R201H (% of mutated)	**# R201L (% of mutated)**	Total # mutated (%)
IM myxoma	19	9 (47)	8 (80)	1 (10)	1 (10)	10 (53)
JA myxoma	4	4 (100)	0	0	0	0

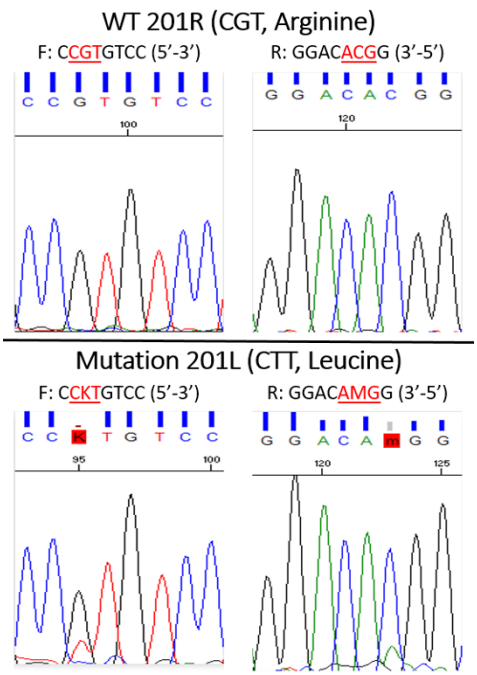

Conclusions: We report the first case of a R201L (arginine to leucine) GNAS mutation identified in IM. Similar to other studies, we identified a significant percentage of cases of IM harboring mutations in GNAS, although we report a higher frequency of R201C mutations. While a R201L mutation has been reported in an individual with MAS, it has yet to be reported in IM or FD. Our study, in addition to others, did not investigate other GNAS mutation hotspots reported in patients with MAS and FD such as codon 227. This raises the possibility that GNAS mutations are more prevalent in IM than currently thought. Further investigation is needed to evaluate IM for other less common GNAS mutations.

41 A Novel Subgroup of Deep Myxoma with Specific Genetic and Histologic Findings and No Evidence of GNAS Mutations: Analysis of Three Cases

Ryan Berry, JIn Wu, Therese Bocklage. University of New Mexico, Albuquerque, NM.

Background: Deep myxomas (intramuscular [IM] and juxta-articular [JA]) are benign tumors that most commonly occur in the deep tissues of the extremities in adults. The tumors may reach a large size but do not undergo malignant transformation. Recurrence risk is minimal for IM but approximately 35% for JA. The two entities may be indistinguishable on histologic review. Point mutations of the GNAS gene are commonly found IM (~40-50%) but are absent in JA. Few cytogenetic findings in deep myxomas have been reported. We recently identified a subset of deep myxomas with increased desmin expression and aberrations of 17q21-22. We performed additional molecular analysis of these cases to better understand them.

Design: Three cases of deep myxomas (2 IM and 1 JA) were identified that showed increased desmin IHC expression and contained alterations of 17q21-22 (Table 1). FISH analysis was performed on these tumors targeting *COL1A1* on 17q22 using BAC clone RP11-267M22 to evaluate for a translocation in this region. *GNAS* mutation analysis of codon 201 exon 8 was performed using PCR and direct sequencing of genomic DNA isolated from FFPE.

	Desmin Expression	**Karyotype**
IM myxoma	75%	t(9;17)(p21;q22) and others
IM myxoma	40%	t(3;17)(q27;q21); del17(q21q25) and others
JA myxoma	10%	add(17)(q21) and others

Results: FISH analysis of *COL1A1* failed to identify a translocation. Evaluation of codon 201 of *GNAS* showed the wild type sequence CTG coding for arginine in all three cases (Figure 1).

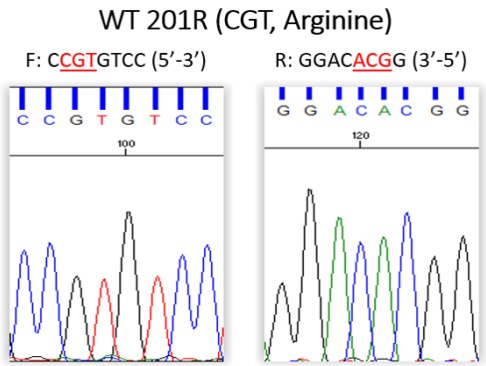

Conclusions: These findings provide further evidence of a genetically distinct myxoid soft tissue tumor with increased desmin expression and aberrations of 17q21-22. FISH analysis of the *COL1A1* gene associated with dermatofibrosarcoma protuberans was negative, excluding a myxoid variant of this entity. The absence of *GNAS* mutations in these cases does not necessarily exclude these tumors being variants of IM myxoma. However, the absence of *GNAS* mutations, the presence of desmin positive fibroblasts and the fact that this unique group comprises cases diagnosed as IM and JA myxoma based on clinical and imaging suggests the possibility of another entity with histologic features overlapping those of IM but with similar indolent behavior.

42 Pediatric Non-Vestibular Schwannomas: A Clinicopathologic Study of 22 Patients

Cory Broehm, Karen Fritchie. Mayo Clinic, Rochester, MN.

Background: While the clinicopathologic features of pediatric vestibular schwannomas, often in the context of neurofibromatosis type 2 (NF2), have been well-studied, there is less data regarding the characteristics of pediatric non-vestibular schwannomas (NVS). Additionally, the rate of SMARCB1/INI1 loss in this population has not been systematically evaluated.

Design: Our institutional archives were searched for cases of NVS arising in patients 18 years or younger. Pathologic characteristics assessed in each case included size of tumor, percent Antoni A and Antoni B tissue, degenerative atypia, calcifications, plexiform architecture, microcystic/reticular growth, mitotic activity, small cell features, and necrosis. Immunohistochemistry for SMARCB1/INI1 protein was performed on a representative block from each case. Clinical information collected included age, sex, location of tumor, and personal/family history of schwannomas or genetic syndromes.

Results: Out of 1960 cases of schwannoma reviewed, 23 pediatric NVS from 9 males and 13 females (age range 5 months to 18 years) were identified; sites included paraspinal (n=10), head and neck (n=6), extremities (n=4), trunk (n=1), mediastinum (n=1) and retroperitoneum (n=1). 21 cases were Antoni A predominant (70 to 100%) with 8 cases comprised solely of Antoni A tissue. 5 cases had plexiform architecture. The mitotic rate of the tumors ranged from 0 to 10/10 high power fields (HPFs), and 3 tumors had mitotic rates of $\geq$ 4 mitoses/10 HPFs. No NVS showed diffuse degenerative atypia, calcifications, microcystic/reticular architecture, small cell features, or necrosis. Two patients had NF2, and both of those patients had multiple NVS. 3 additional patients had multiple NVS. Followup was available in 21 patients (range 1 week to 194 months), and 4 patients (1 NF2, 3 non-NF2) experienced a recurrence or developed additional NVS. All tumors (23/23) showed retained nuclear expression of SMARCB1/INI1.

Conclusions: Pediatric NVS are uncommon and seem to have a relatively homogeneous appearance, with little histomorphologic variability, and a predominance of Antoni A areas. Pathologists should be aware that schwannomas in this age group may be cellular with mitotic rates $\geq$4/10 HPFs to avoid misclassification as spindle cell sarcoma. Loss or mosaicism of SMARCB1/INI1 appears uncommon in this subset of tumors, but a larger series is needed to confirm these findings.

43 Extraosseous, Extradural Chordomas of the Spine: A Unique Chordoma Subset

Jodi M Carter, Doris E Wenger, Carrie Y Inwards. Mayo Clinic, Rochester, MN.

Background: Chordomas are malignant tumors derived from the embryologic notochord. The vast majority arise within the bones of the skull base and spine. While chordomas arising in extraspinal bone and soft tissues have been described, there are only rare case reports of extradural chordomas in the radiology and neurosurgery literature, and none in the pathology literature. We report our experience, over the past two decades, with six cases of extraosseous, extradural chordomas presenting with a unique clinicoradiologic profile.

Design: Six cases of extraosseous, extradural chordoma were retrieved from our institutional archives. Clinical history, radiologic studies and histologic slides were evaluated. Clinical follow-up was obtained from the medical record. On available material, immunohistochemistry for cytokeratins and brachyury was performed.

Results: Tumors occurred primarily in adults (3 females, 2 males; median 52y, range 44-58y) and in one 12y male. Several patients presented with unilateral back pain and/or radiculopathies at the involved spinal level. In all cases, advanced imaging revealed a lesion closely mimicking a benign neurogenic tumor, composed of a unilateral enhancing extradural mass (mean 2 cm), expanding and extending through neural foramina within the cervical (N=4) or lumbar (N=2) spine. No case showed intraosseous extension. All tumors were surgically excised (2 with a pre-operative diagnosis of chordoma), with variable surgical margins. One patient received adjuvant external beam radiotherapy and two patients received proton beam therapy. Histologically, all 6 tumors showed typical features of conventional chordoma including epithelioid, vacuolated cells with variable amounts of eosinophilic cytoplasm, forming cords and nests, embedded in a myxoid matrix. In tested cases, the neoplastic cells uniformly expressed wide-spectrum cytokeratins (N=6) and brachyury (N=4). With mean follow-up of 6.4y, (range 1-20y), one patient had local residual/recurrent disease within 1 year. The other 5 patients are disease-free.

Conclusions: We report the first series of extraosseous, extradural chordomas. This rare subset of chordoma has a distinctive and misleading clinicoradiologic profile, closely resembling a benign neurogenic tumor. It is important for pathologists to be aware of this entity to avoid a mistaken diagnosis of soft tissue tumors more commonly seen in this setting, and to guide the appropriate oncologic management indicated for chordomas.

44 Identification of Novel Gene Fusion FUS-CREM in Clear Cell Sarcoma of Soft Tissue by Anchored Multiplex Polymerase Chain Reaction

Kenneth Chang, Angela Goytain, Xiu Qing Wang, Tracy Tucker, Amy Lum, Stephen Yip, Torsten O Nielsen, Tony Ng. KK Women's and Children's Hospital, Singapore, Singapore; Duke-NUS Graduate Medical School, Singapore, Singapore; University of British Columbia, Vancouver, BC, Canada; BC Cancer Agency, Vancouver, BC, Canada; Vancouver General Hospital, Vancouver, BC, Canada.

Background: Gene fusions *EWSR1-ATF1* and *EWSR1-CREB1* have been identified in CCS, identification of which is often crucial in distinguishing CCS from malignant melanoma. Anchored multiplex polymerase chain reaction (AMP) is a next-generation sequencing-based technique in which gene fusions can be identified in a PCR-based assay for which there are sarcoma-targeted panels available (Archer FusionPlex Sarcoma Panel™). This assay has discovery potential, as it utilizes primers targeting only one fusion partner, while the other partner is identified through next-generation sequencing agnostic of the identity and breakpoint of the binding partner. We describe a novel gene fusion *FUS-CREM* in a CCS which was identified by AMP.

Design: The patient was a 55 year old male with a thigh mass. Morphology and immunohistochemistry supported a differential diagnosis of CCS versus malignant melanoma, and *EWSR1* FISH was performed during initial diagnostic work-up. AMP was performed on this case as part of a validation study of the technology platform in sarcoma diagnostics. We also performed FISH utilizing a *FUS* breakapart probe, and RT-PCR with primers for *FUS* and *CREM*. A series of 8 additional *EWSR1*-intact melanocytic tumors in which CCS was a differential diagnosis were further assessed by FISH and RT-PCR for the *FUS-CREM* fusion.

Results: Initial *EWSR1* FISH showed a complex polyploidy result with no *EWSR1* gene rearrangement identified. AMP demonstrated a novel *FUS-CREM* fusion, with the fusion junction between *FUS* exon 8 and *CREM* exon 7. FISH confirmed a rearrangement of the *FUS* locus, and RT-PCR demonstrated an amplicon across the exon 8-exon 7 breakpoint. This finding is biologically justified by the homology between *CREM* and *CREB1*, both representing cyclic AMP-responsive element modulators. Amongst the 8 additional CCS cases studied, no further cases showed the *FUS-CREM* gene fusions.

Conclusions: *FUS* can replace *EWS* in CCS. We identify a novel gene fusion *FUS-CREM* in CCS using the AMP technique, adding to the list of known gene fusions characterizing CCS. We also show that a targeted next-generation sequencing-based assay such as AMP has the capability of discovering novel gene fusions in which only one fusion partner is covered in the primer pool. Such assays are of increasing diagnostic utility with the ongoing discovery of novel gene fusions and fusion variants.

45 Histopathology of So-Called Synovial Cysts of the Lumbar Spine

Ivan Chebib, Connie Y Chang, Darcy A Kerr, Vikram Deshpande, G Petur Nielsen. Massachusetts General Hospital and Harvard Medical School, Boston, MA; University of Miami Miller School of Medicine, Miami, FL.

Background: "Synovial cysts" of the lumbar spine are a feature of degenerative arthropathy of facet joints of the lumbar spine. The histogenesis of these specimens is uncertain as many lack true synovial-lining, as would be expected for cysts derived from diarthordial joints. The purpose of this study was to further characterize the histologic findings of specimens submitted as lumbar "synovial cysts".

Design: The laboratory information system was searched for lumbar "synovial cyst" from 2012-2015. The histologic slides were reviewed with special stains, if available, and the presence/absence of the following histologic features was evaluated: evidence of cyst histologically and type of lining; presence of ligamentum flavum (LF); type of cyst contents (fibrinoid, myxoid, bloody); presence of calcification and type (dystrophic – coarse or finely granular basophilic debris, or calcium pyrophosphate).

Results: Seventy five cases of lumbar "synovial cysts" were reviewed: 54% females, average age 64 (range 50-89) and 46% males, average age 69 (range 51-83). Thirty-one of 75 lumbar cysts (41%) were lined by synovium, at least focally, consistent with synovial cysts. Thirty-six (48%) lumbar cysts lacked synovial lining. Of these, 28/36 cases contained fragments of LF with pseudocyst formation (cystic degenerative changes) and 8/36 showed fibrous-walled pseudocysts without LF. In the remaining 8 patients, no cyst wall was identified histologically. There were 25 cases that had fibrinoid cyst contents (7 synovial cysts, 11 degenerated LF, 4 pseudocysts without LF, 3 cases without cyst walls), 5 cases with myxoid contents (3 degenerated LF, 2 cases without cyst walls) and 17 cases of mixed fibrinoid/myxoid cyst contents (5 synovial cysts, 10 degenerated LF, 2 cases without cyst walls). Twenty cases (1 synovial cyst, 15 degenerated ligamentum flavum, 4 cases without cyst walls) contained peculiar finely granular basophilic material (staining with von Kossa, when performed) and surrounding foreign-body giant cell reaction, resembling calcifications seen in tumoral calcinosis.

Conclusions: So-called lumbar "synovial cysts" manifest a range of histologic findings and comprise both synovial-lined cysts and non-synovial pseudocysts, often cystically degenerated ligamentum flavum, that may contain finely granular tumoral calcinosis-like calcifications.

46 Diagnostic Utility of IDH1/2 Mutation To Distinguish Dedifferentiated Chondrosarcoma from Undifferentiated Pleomorphic Sarcoma

Shaoxiong Chen, Karen Fritchie, Shi Wei, Kendra Curless, Kristin Post, Liang Cheng. Indiana University, Indianapolis, IN; Mayo Clinic, Rochester, MN; The University of Alabama at Birmingham, Birmingham, AL.

Background: Histologically, it is impossible to distinguish dedifferentiated chondrosarcoma (CHS) from undifferentiated pleomorphic sarcoma (UPS) of the soft tissue. In this study, we sought to evaluate whether an *IDH1* or *IDH2* mutation signature could be used as a clinically diagnostic marker for distinguishing these two lesions.

Design: Cases of dedifferentiated CHS and UPS were collected from Indiana University, Mayo Clinic and University of Alabama at Birmingham. H. E. slides were re-examined and diagnoses were confirmed. DNA was extracted from unstained slides cut from formalin fixed paraffin embedded tissues. *IDH1/2* mutation analysis was performed using the Qiagen *IDH1/2* RGQ PCR Kit, which detected multiple mutations in codon 132 of the *IDH1* gene and codon 172 of the *IDH2* gene, respectively.

Results: Among 23 cases of dedifferentiated chondrosarcoma,18 each harbored one somatic mutation in either *IDH1* or *IDH2*. Specifically, they were 5 R132C, and 4 R132 mutations in *IDH1* gene and 9 R172 mutations in *IDH2* gene. Interestingly, two cases each contained mutations in both *IDH1* and *IDH2*. They are *IDH1* R132 and *IDH2* R172 in one case and *IDH1* R132H and *IDH2* R172 in the other case. Among 24 cases of UPS of the soft tissue, no mutations were detected in the *IDH1* or *IDH 2*.

Conclusions: Overall, 20/23 (87%) dedifferentiated CHS cases contain at least one mutation in either *IDH1* or *IDH2*. Our study shows higher mutation rate compared to one previous study 13/23 (56.5%) in the dedifferentiated CHS. Identification of *IDH1* or *IDH2* mutation strongly supports the diagnosis of dedifferentiated CHS rather than UPS. This finding also gives some insight into the pathogenesis of these two diseases and might lead to the development of molecular-targeted therapy for dedifferentiated CHS.

47 Ewing Sarcoma (ES) with ERG Gene Rearrangements: A Molecular Study Focusing on the Prevalence of FUS-ERG and Common Pitfalls in Detecting EWSR1-ERG Fusions by FISH

Sonja Chen, Kemal Deniz, Yun-Shao Sung, Lei Zhang, Sarah M Dry, Cristina Antonescu. Memorial Sloan Kettering Cancer Center, New York, NY; Erciyes University, Kayseri, Turkey; UCLA, Los Angeles, CA.

Background: The genetics of ES are characterized by a canonical fusion involving *EWSR1* gene and a member of ETS family of transcription factors, such as *FLI1* and *ERG*. In fact *ERG* gene rearrangements represent the second most common molecular alteration, with *EWSR1-ERG* being identified in 5-10% of cases and only a handful of reports documenting a *FUS-ERG* fusion.

Design: In this study, we focus on ES with *ERG* gene abnormalities, specifically investigating the prevalence and clinico-pathologic features of *FUS-ERG* fusions in a large cohort of small blue round cell tumors (SBRCTs) and comparing them to the 8 *FUS*-positive ES from the literature.

Results: Among the 80 SBRCTs tested, 6 (7.5%) cases harbored *FUS* gene rearrangements; 5 showing fusion to *ERG* and one to *FEV*. All patients except one were females, with a mean age 38 years (range 13-46); 4 being located in bone and 2 in soft tissue. We further identified a number of ES with *ERG* gene rearrangements by FISH lacking both *EWSR1* and *FUS* abnormalities. In one case RNA sequencing performed showed an *EWSR1-ERG* transcript despite lack of *EWSR1* rearrangements by FISH. Additional 3-color FISH fusion assay demonstrated the fusion of *EWSR1* and *ERG* signals in the 4 cases negative for break-apart *EWSR1*. These masked fusions occur as *EWSR1* and *ERG* have oposite orientations, requiring a complex rearrangement and subsequent inversion for the functional transcript to form.

Conclusions: This is the first molecular investigation to establish the prevalence of *FUS* gene rearrangements in a well-characterized cohort of SBRCT, accounting for 7.5% of cases lacking all other known fusions. The most common *FUS* gene partner is *ERG*, with very infrequent cases showing *FEV* involvement. *FUS-ERG* positive SBRCTs show a monotonous phenotype and strong CD99 membranous immunoreactivity, which are similar to classic ES. Our study also highlights a significant pitfall in the setting of

EWSR1-ERG fusion, where FISH assay did not detect *EWSR1* rearrangements in half of the cases due to the complex pattern of t(21;22). In cases with classic morphologic appearance and/or strong CD99 and ERG immunoreactivity, additional molecular testing should be applied, such as *ERG* FISH or RT-PCR/NGS, for a definitive diagnosis. Although our study group is limited there were no clinical, morphologic and immunoprofile differences noted among the various subsets of *ERG*-rearranged SBRCTs.

48 MDM2 and CDK4 Immunohistochemistry Is Inadequate in the Diagnosis of Problematic Low-Grade Lipomatous Tumors: A Follow-Up Study

Michael Clay, Anthony Martinez, Mark A Edgar. Emory University Hospital, Atlanta, GA.

Background: Immunohistochemistry (IHC) has been promulgated as a surrogate marker for fluorescent in situ hybridization (FISH) testing in atypical lipomatous tumor/well differentiated liposarcoma (ALT/WDL). However, this has not been validated in a large series of cases with either bland or borderline histologic features that specifically could not have been diagnosed based on H&E staining alone. We have evaluated the utility of IHC for MDM2 and CDK4 in borderline cases with known *MDM2* FISH results.

Design: Immunohistochemical staining for MDM2 and CDK4 was performed in 210 low-grade lipomatous tumors with known FISH results. 27 cases were removed secondary to scant tissue on stained slides or poor staining quality (uninterpretable), leaving 183 cases (56 ALT/WDLs and 127 lipoma/lipoma variants). Two pathologists blinded to the FISH results scored the slides, with discrepant cases discussed and consensus reached. Each stain was considered positive if >10% of tumor nuclei displayed 1+ nuclear staining, or if >5% of tumor nuclei displayed 2-3+ intensity.

Results: We observed expected non-specific staining of histiocytes and endothelial cells. A number of cases also showed false positive staining of tumor nuclei (n=9, 2 pleomorphic lipomas, 7 lipomas), some of which was strong and diffuse (up to 75% of tumor nuclei). 28 cases exhibited very rare faint staining (1-5%, 1+). These were considered negative at the time of interpretation, and a retrospective review indicated these cases were typically negative by FISH (24 of 28 cases, 85%). The test characteristics can be seen in table 1.

	MDM2 IHC		CDK4 IHC		Used in Combination
	Positive	Negative	Positive	Negative	
Lipoma	2	125	7	105	
ALT/WDL	26	30	20	30	
Sensitivity	46%		40%		48%
Specificity	98%		94%		94%
PPV	93%		74%		77%
NPV	81%		78%		80%

IHC: immunohistochemistry; ALT/WDL: atypical lipomatous tumor / well-differentiated liposarcoma; PPV: positive predictive value; NPV: negative predictive value

Conclusions: IHC is insufficiently sensitive for routine diagnosis of diagnostically challenging lipomatous tumors. Higher sensitivity in previous studies likely results from greater cellularity than was present in our paucicellular lipoma-like cases, but it is in these latter cases that ancillary testing is most needed. In histologically bland and borderline adipocytic tumors, FISH for *MDM2* gene amplification should be the first line ancillary test.

49 HER3 (erbB3) as a Potential Therapeutic Target in Peripheral Nerve Sheath Tumors (PNST): In Vitro and In Vivo Models

Sherley Diaz, Javier Hernandez Losa, Joan Castellsague, Claudia Valverde, Roso Mares, Angel Garcia, Cristina Teixido, Teresa Moline, Juana Fernandez-Rodriguez, Eduard Serra, Alberto Villanueva, Santiago Ramon y Cajal, Conxi Lazaro, Cleofe Romagosa. Vall d'Hebron University Hospital, Barcelona, Spain; Hereditary Cancer Program, Institut Català de Oncologia, Barcelona, Spain; Institut de Medicina Predictiva i Perzonalitzada del Cancer, Barcelona, Spain.

Background: Malignant peripheral nerve sheath tumors (MPNST) comprise 5-10% of sarcomas. Prognosis is poor and the search for new treatments is ongoing. HER3 is a crucial receptor for neuregulin signalling in Schwann cells. Our aims were to determine the prevalence of HER3 receptor expression in MPNST, and to evaluate the impact of HER3 inhibition in a subgroup of mesenchymal tumor cell lines and orthotopic xenograft mouse models.

Design: HER3 expression was immunohistochemically assessed in 121 mesenchymal tumors, including 16 neurofibromas, 16 schwanomas, 14 MPNST and 75 other spindle lesions. HER3 expression was also evaluated by western blot in 5 mesenchymal cell lines including RT4 (murine schwann cells) and JHM (sporadic MPNST). HER3 expression was inhibited by the infection with specific short hairpin RNA in all of them. Finally we test MEHD7945A (HER1/3 inhibitor), pertuzumab (HER2/3 inhibitor) and lapatinib (HER1/2 inhibitor) against two patient derived MPNST (one NF1 patient and other sporadic) orthotopically transplanted into nude mice. Her1/2/3 were previously evaluated by immunohistochemistry and western blot in both orthotopic models.

Results: HER3 overexpression was found in 31% of cases. Significantly, HER3 positivity was present in 50% MPNST. Moreover, HER3 expression was found to be overexpressed in 4 of the 5 cell lines studied. Their stable knockdown of HER3 expression induced a decreased of proliferation rate in all the Her3 positive cell lines. Low levels of HER3 expression were observed in the NF1 associated orthotopic tumor while it was overexpressed in the sporadic one. Her1/2 showed similar results in both models. Clear differences in size -changes and necrosis were observed between *in vivo treated* and non-treated tumors in the sporadic orthotopic tumor (Her3+), but not in the NF1-associated one (Her3-).

Conclusions: HER3 overexpression is frequently found in MPNST. Genetic and pharmacologic approaches to blockade Her3 in MPNST are able to prevent tumor growth only in the subgroup of tumors overexpressing Her3. These results support the rationale of the use of Her3 inhibitors/monoclonal antibodies as new therapeutic approaches for the treatment of MPNST.

50 KDM2B—Setting the Stage for Aberrant Silencing in Synovial Sarcoma

Amanda R Dancsok, Ana Banito, Scott Lowe, Torsten O Nielsen. University of British Columbia, Vancouver, BC, Canada; Memorial Sloan Kettering Cancer Center, New York, NY.

Background: Recent studies have highlighted a critical role for epigenetic dysregulation in synovial sarcoma, which may be potentially targetable with drugs under active development. Synovial sarcoma occurs in part as a result of tumor suppressor gene silencing via histone-3-lysine-27 (H3K27) trimethylation. This silencing is brought about by the disease's pathognomonic fusion oncoprotein, SS18-SSX, which links DNA-binding transcription factor ATF2 to gene-silencing complex PRC2; however, the epigenetic background of synovial sarcoma likely involves other cofactors.

Our group, using a high throughput shRNA screen for epigenetic cofactors, identified *KDM2B* as a gene as critical to synovial sarcoma growth as *SS18-SSX*. KDM2B is a histone demethylase specific to histone-3-lysine-36 (H3K36). Recent work suggests that H3K36 methylation prevents PRC2-mediated H3K27 methylation, explaining why KDM2B might be necessary for SS18-SSX-driven tumor suppressor silencing. We recently confirmed high *KDM2B* mRNA expression in synovial sarcoma cell lines, and found that knockdown of SS18-SSX induces KDM2B protein depletion; however, the role of KDM2B in synovial sarcoma has not yet been confirmed in patients.

Design: KDM2B immunohistochemistry was performed on paraffin-embedded tissue microarrays containing samples from 57 human synovial sarcomas. For comparison, staining was also done on arrays containing over 200 other soft tissue neoplasms: translocation-associated sarcomas, other sarcomas, and benign mesenchymal tumors. Results were linked to treatment and outcome data.

Results: KDM2B gave easily interpretable, strong nuclear staining in all synovial sarcoma cases. A mean of 54% of synovial sarcoma cells were positive (95%CI 51-57), significantly higher (p=0.0002) than the combined mean across other neoplasms studied, among which benign nerve sheath tumors and melanomas also showed relatively high expression. In synovial sarcoma, high expressors of KDM2B had improved overall survival at 15 years, with a hazard ratio of 0.11 at the optimized cutpoint of 82% expression. Monophasic histologies had significantly higher expression than biphasic (59% vs. 38% of sarcoma nuclei).

Conclusions: This data demonstrates that KDM2B, a potential therapeutic target for new epigenetic modifying drugs, is commonly and highly expressed in patient synovial sarcoma specimens. This work adds to an emerging body of evidence for a role of KDM2B and epigenetic dysregulation in the oncogenesis of synovial sarcoma.

51 Identification of Recurrent Copy Number Alterations Specific to the De-Differentiated Component of Liposarcoma, Using Capture-Based Next Generation Sequencing (NGS)

Brianne H Daniels, Daniel E Roberts, Nancy Joseph, Andrew E Horvai. University of California San Francisco, San Francisco, CA.

Background: Well-differentiated liposarcoma (WL) is the most common soft tissue sarcoma in adults. WL provides a unique model of sarcoma progression, in that "dedifferentiation" of WL to a non-lipogenic, or dedifferentiated, liposarcoma (DL) is well-documented. WL and DL demonstrate amplification of chromosome region 12q13-15 but the mechanism of progression from WL to DL is unclear. Increased activity of AP1 signaling has been proposed as a mechanism in some cases. In the present study, we compared single nucleotide variants (SNVs), small insertions or deletions (Indels), and copy number alterations (CNAs) between matched lipogenic and non-lipogenic components of DL.

Design: Ten DL with matched normal, lipogenic and non-lipogenic components were selected. DNA was extracted from formalin-fixed paraffin embedded tissue. Capture-based next generation sequencing (NGS) was performed targeting the coding regions of over 500 cancer genes as well as select introns, covering a total of 2.8 Megabases (MB).

Results: Average sequencing depth was 635 unique reads per interval. No recurrent SNVs or small Indels were identified that could account for progression, including in AP1 signaling pathway genes. There was also no difference in mutational burden between matched lipogenic and non-lipogenic pairs (2.9 mutations/MB and 3.1 mutations/MB, respectively).

Recurrent CNAs were identified, including the expected amplification of 12q15 (*MDM2*) and 12q13.3 (*CDK4*) in both components of all 10 cases. Amplification of 6q23 (*MAP3K5*) was also seen in matched lipogenic and non-lipogenic components in 4 of 10 cases. Several CNAs were more frequent in non-lipogenic components, including amplifications of 1p31 (*JUN*), 11p12 (*RRAS2*), and 8q21 and deletions of distal 18q, 10q (*PTEN*), distal 11q and 3q21-22.

	Amplifications			Deletions			
	1p31 (JUN)	*11p12 (RRAS2)*	*8q21*	*distal 18q*	*10q (PTEN)*	*distal 11q*	*3q21-22*
Lipogenic	1	0	0	0	0	0	0
Non-lipogenic	5	4	3	4	3	3	3

Conclusions: Recurrent mutations and overall mutational burden do not account for liposarcoma progression. However, copy number alterations in chromosomal regions containing *MAP3K5*, *JUN, PTEN* and possibly other pathways may account for progression in a subset of cases. Further study, including pathway analysis, will shed additional light on the genetic changes driving progression.

52 Correlation of Histological Grade of Dedifferentiation with Clinical Outcome in 51 Cases of Dedifferentiated Liposarcomas

Kossivi E Dantey, Oleksandr Yergiyev, Karen Schoedel, Uma Rao. University of Pittsburgh Medical Center, Pittsburgh, PA.

Background: Well-differentiated liposarcomas are low-grade, locally recurrent tumors in deep soft tissue and retroperitoneum that can dedifferentiate and have greater potential for local recurrence and metastases. We correlated grade of dedifferentiation with survival in 51 cases of resected dedifferentiated liposarcoma (DLPS) retrieved over a 19-year period. Follow up was available in 48 patients ranging from 2 months to 19 years (median 36 months).

Design: The neoplasms were morphologically classified into 2 groups. The first group was composed of DLPS with a pleomorphic and spindle cell component (HGDLPS n=30); that included foci of smooth muscle differentiation (12) and osteosarcoma (4), in addition to DLPS with myxoid areas and a slightly plexiform vascular pattern (n=9) (total n=39). The second group included 12 patients with DLPS showing a low-grade spindle cell component with less than 5 mitosis per 10 high-power fields and little or no necrosis (LGDLPS, outcome was available in 9 patients). The majority of tumors had an intra-abdominal location (retroperitoneum n=30, thigh n=11, spermatic cord n= 3, arm n=3, pelvis n= 2, mediastinum n=1, and neck n=1). Among the 2 groups, the retroperitoneum was the most common tumor site. Most of the tumors were large (mean= 21 cm, range=2.7-65cm). Due to the small sample size, testing was performed using Fisher's exact test. Results of fluorescent in situ hybridization (FISH) performed on selected cases and clinical data were reviewed.

Results: Twenty-one out of 39 patients with HGDLPS and DLPS with myxoid areas (54%) died of tumor. One patient out of 9 died in the LGDLPS group (11%) (Fisher's exact test, p=0.022, one-tailed). Metastasis (n=4) occurred only in the HGDLPS cases and was independent of type of differentiation. MDM2 amplification was present in all evaluated cases by FISH (HGDLPS, 14; DLPS with myxoid areas,4 and; LGDLPS, 7). The 7 cases of DLPS with myxoid areas on which DDIT3 studies were performed did not demonstrate the characteristic DDIT3 break apart pattern.

Conclusions: Among the 2 groups, patients with LGDLPS had a significantly better outcome with regard to metastases and survival. The DLPS with myxoid areas closely resembled myxoid LPS. However, myxoid LPS are uncommon in the retroperitoneum and FISH did not show the characteristic DDIT3 break apart pattern. Distinction between the different groups of DLPS can have important clinical implications.

53 Utility of SATB2 as a Quality Control Indicator in Osteosarcoma Tissue Microarray

Elizabeth G Demicco, Jen-Wei Tsai, Davis Ingram, Wei-lien Wang. Mount Sinai Hospital, New York, NY; The University of Texas M. D. Anderson Cancer Center, Houston, TX.

Background: Although the use of tissue microarray (TMA) is widely accepted for high throughput evaluation of immunohistochemical biomarkers in formalin-fixed paraffin embedded specimens, expression of markers may be affected by external factors such as fixation time, block storage conditions, and decalcification, among others. In order to identify factors affecting the reliability and antigenicity of an osteosarcoma (OSA) TMA, we evaluated expression of SATB2, a sensitive marker of osteoblastic differentiation, which has been reported to be expressed in 100% of skeletal OSA.

Design: TMA was constructed to include 240 pairs of 1 mm cores from 224 OSA of skeletal origin, representing 174 distinct tumors from 143 patients. Immunohistochemical study for SATB2 was performed. Any nuclear staining of OSA cells was scored as positive. Comparisons were analyzed using Fisher exact test, and risk ratio (RR) calculated.

Results: SATB2 expression was evaluable in 227 samples, including 71 primary biopsies (PB), 99 primary resections (PR), 35 metastases, and 22 local recurrences (LR). Nuclear SATB2 expression was present in 69% of samples, including 86% of PB, 55% of PR, 77% of LR, and 69% of metastases. Cores showing any chondroblastic differentiation were frequently negative for SATB2, with loss in 42% of cases vs. 29% of cores without malignant cartilage. Of 13 PR with 2 pairs of cores from histologically distinct regions, 6 were positive in one region and negative in the other, 4 were negative in both and 3 were positive in both.

Negative SATB2 expression correlated with lack of osteoid matrix on TMA core (RR 1.535, p=0.038), prolonged decalcification (RR 2.319, p=0.0003), tumor viability of <10% (RR 1.932, p=0.04), history of pre-operative chemotherapy (RR 2.257, p<0.0001), and PR vs. PB (RR 3.227, p<0.0001). While 27/30 PB were positive for SATB2 (90%), only 18 (55%) of the matched post therapy PR retained expression. No change in expression was seen in 7 paired PB and untreated PR specimens. SATB2 expression did not vary with case age.

Conclusions: SATB2 expression may be heterogenous within OSA, with least frequent expression in chondroblastic foci. Tumor heterogeneity may preclude utility of SATB2 as a quality control marker for TMA staining.

Factors affecting SATB2 expression in resection specimens are favored to include biologic loss due to low tumor viability or effects of preoperative chemotherapy, although tissue processing artifacts, such as over-decalcification or fixation may also play a role.

54 Mutations in Histone H3.3 Variants in Giant Cell Tumor of Bone

Brendan C Dickson, Leonie G Mikael, Tenzin Gayden, Ashot Harutyunyan, Simon Papillon-Cavanagh, Jacek Majewski, Nada Jabado, Jay S Wunder. Mount Sinai Hospital, Toronto, ON, Canada; McGill University, Montreal, QC, Canada.

Background: Giant cell tumor of bone (GCT) is a benign, albeit locally aggressive, neoplasm associated with a high rate of local recurrence. Tumors predominate in young adults, encompass a broad anatomic distribution, and may be associated with significant morbidity. The disease-defining mutation in GCT frequently involves histone 3.3 (*H3F3A*), with most cases associated with G34W, and rare cases with G34L, G34V, G34R and G34M mutations. There remains a minority of cases with a hitherto unreported underlying driver alteration; as a result, we sought to analyze our own patient population for histone *H3F3A* mutations.

Design: Cases were re-reviewed to confirm the diagnoses. Using digital droplet PCR (ddPCR) we analyzed 23 consecutive GCTs for *H3F3A* mutations. Briefly, formalin fixed paraffin-embedded tissue was cut into 10 micron sections, treated with deparaffinization solution and DNA extracted. ddPCR was performed according to standard methods with primers and probes specific for G34W and mutant allele frequency was calculated. Samples that did not carry G34W mutation in H3F3A were analyzed by Whole Exome Sequencing using Illumina Nextera Rapid Exome.

Results: A driver mutation in histone H3.3 was identified in 100% of cases, with the vast majority being in H3F3A G34W (82.6%), and minor incidence for G34L (8.7%) and G34V (4.3%). We also identified an additional alternate mechanism affecting H3.3 in the sample that was wildtype for G34 H3.3.

Conclusions: Elucidation of the genetic alterations in GCT offers the potential for both refined diagnostic capabilities for pathologists, as well as potential therapeutic targets. We confirm the high prevalence of the G34W mutation in GCT. Our results also highlight the presence of G34L and G34V mutations in a minority of cases. We conclude alterations in H3.3 drive virtually all GCT. Additional studies are warranted to describe the functional impact of these G34XH3.3 alterations in the genesis of GCT.

55 A Subset of Epithelioid Sarcomas with Intact INI1 (SMARCB1) Is Deficient for SMARCA4 and SMARCA2

Leona A Doyle, Christopher Fletcher, Jason L Hornick. Department of Pathology, Brigham and Women's Hospital, Harvard Medical School, Boston, MA.

Background: Approximately 5% of epithelioid sarcomas, both conventional and proximal types, show intact INI1 (SMARCB1) expression by immunohistochemistry (IHC). Little is known about the molecular genetics of this small subset of epithelioid sarcomas. SMARCA4 is the ATPase subunit of the SWI/SNF chromatin-remodeling complex. Recently, *SMARCA4* mutations were identified in ovarian small cell carcinoma of hypercalcemic type, some undifferentiated thoracic sarcomas with epithelioid or rhabdoid features, and a small subset of malignant rhabdoid tumors (with intact INI1 expression). Corresponding loss of SMARCA4 protein expression and concomitant loss of SMARCA2 (another member of the SWI/SNF complex) are also seen in these tumor types. The goal of this study was to determine if SMARCA4/SMARCA2 deficiency was present in epithelioid sarcomas with intact INI1 expression.

Design: 15 cases of epithelioid sarcoma with intact INI1 expression, but otherwise typical morphologic and immunohistochemical features, were identified (9 conventional type, 6 proximal type). IHC for SMARCA4 and SMARCA2 was performed on whole tissue sections; expression was considered deficient when tumor cells lacked nuclear staining in the presence of nuclear reactivity in non-neoplastic cells, which served as internal controls. Clinical and histologic features were also reviewed.

Results: 2 cases showed loss of both SMARCA4 and SMARCA2 expression. Both tumors arose in males (40 and 61 years of age), one in a paraesophageal/mediastinal location and the other in retroperitoneum; the latter patient also had a larger pleural-based mass and a smoking history. Tumors were composed of sheets of large, monomorphic epithelioid cells with abundant amphophilic or palely eosinophilic cytoplasm and round nuclei with prominent nucleoli, and showed extensive tumor necrosis. Focal rhabdoid features were seen in one case. Both tumors expressed keratins, EMA and CD34. Both patients had metastases at the time of presentation.

Conclusions: A subset of proximal-type epithelioid sarcomas with intact INI1 expression is deficient for SMARCA4 and SMARCA2. These tumors show significant overlap with the recently described 'SMARCA4-deficient thoracic sarcomas', distinguished from proximal-type epithelioid sarcoma only by intact INI1 expression and loss of SMARCA4/SMARCA2, the latter due to somatic *SMARCA4* mutations.

56 Histone 3.3 Mutations in Giant Cell Tumor and Giant Cell-Rich Sarcomas of Bone

Alessandro Franchi, Alberto Righi, Marco Gambarotti, Piero Picci, Angelo Paolo Dei Tos, Lisa Simi, Irene Mancini. University of Florence, Florence, Italy; Rizzoli Institute, Bologna, Italy; Treviso Regional Hospital, Treviso, Italy.

Background: Mutually exclusive histone 3.3 gene mutations have been recognized in chondroblastoma and giant cell tumor of bone (GCTB), which may be useful for differential diagnostic purposes in morphologically ambiguous cases. While over 90% of GCTB presents histone 3.3 variants exclusively in the *H3F3A* gene, chondroblastoma is mutated mainly in *H3F3B*.

Design: In this study we examined a series of giant cell rich primary bone tumors, aiming to evaluate the possible diagnostic role of histone 3.3 mutations in the differential diagnosis between GCTB and giant cell rich sarcomas. Fifteen cases of GCTB and 15 giant cell-rich sarcomas (8 osteosarcomas and 7 undifferentiated pleomorphic sarcomas) were selected from our institutional archives. Eight chondroblastomas were used as controls. Direct sequencing for the presence of *H3F3A* and *H3F3B* variants in coding region between codons 1 and 42, including the hot spot codons (28, 35 and 37) was performed on DNA extracted from formalin-fixed paraffin-embedded tissue.

Results: Fourteen GCTs (93.3%) presented a mutation in the *H3F3A* gene (11 G35W, 1 G35V, 1 G35M and 1 G35E). In the group of sarcomas, we identified two variants. One was a G35E in a secondary malignant GCTB, which developed after 4 local relapses of a GCT of the sacrum, and the second was a G35W in a giant cell rich osteosarcoma. No mutation was identified in the *H3F3B* gene in the group of GCTB and giant cell-rich sarcomas, whereas all the chondroblastoma tested presented a K73M variant.
Conclusions: Our results confirm that H3F3A mutations occur with high frequency in GCTB, while they are seldom found giant cell rich sarcomas of bone arising de novo. Thus, *H3F3A* mutational testing may be a useful adjunct to differentiate GCTB from giant cell rich sarcomas.

57 Detection of Sarcoma Oncogenic Fusion Transcripts Using ArcherTM Sequencing Technology

Caleb Ho, Kerry Mullaney, Catherine OReilly, George Jour, Purvil Sukhadia, Lu Wang, Michael F Berger, Maria E Arcila, Marc Ladanyi, Meera Hameed, Ryma Benayed. Memorial Sloan Kettering Cancer Center, New York, NY; University College Cork, Cork, Ireland; MD Anderson Cancer Center, Houston, TX.
Background: Fluorescence in-situ hybridization (FISH),karyotyping,and RT-PCR are common oncogenic fusion gene detection methods,but each has its disadvantages. Archer™,a RNA-based next-generation sequencing assay,allows targeted oncogenic fusion transcript detection without knowledge of the corresponding fusion partners or breakpoints. In this study,we compared the performance of Archer™ to other methods in various sarcomas with well-characterized fusion genes.
Design: RNA extracted from 18 FFPE sarcomas were tested with the Archer™ Fusion Plex Sarcoma assay panel. Amplified products from Archer's Anchored Multiplex PCR™ enrichment were sequenced on the Illumina MiSeq™ platform and analyzed on the Archer™ analysis pipeline. The findings were compared to available IHC,FISH and RT-PCR results.
Results: ASPSCR1-TFE3 fusions with identical breakpoints were detected in all 4 Alveolar Soft Part Sarcomas (positive for TFE3 by IHC). In contrast, NAB2-STAT6 fusions with variable breakpoints were found in all 5 Solitary Fibrous Tumors. Each of 3 Ewing Sarcomas showed a different EWSR1 fusion partner (ERG, FLI1 and ETV4). SS18-SSX1 fusions were found in 2 Synovial Sarcomas (both strongly positive for TLE1 by IHC). In one case, Archer™ provided valuable diagnostic information,as FISH using SS18 break-apart probes showed loss of 3' signal,which was suggestive but not diagnostic of gene rearrangement,while SS18-SSX RT-PCR failed to show the fusion transcript. Other detected fusion transcripts included EWSR1-WT1 (Desmoplastic Small Round Cell Tumor,2 cases),TAF15-NR4A3 (Extraskeletal Myxoid Chondrosarcoma,1 case),and EWSR1-CREB3L1 (Hybrid Low grade Fibromyxoid Sarcoma/Sclerosing Epithelioid Fibrosarcoma,1 case). In summary,Archer™ detected all fusion genes identified by RT-PCR and/or FISH. In addition,it also identified fusion transcripts in cases for which corresponding PCR primers or FISH probes were not available for diagnostic uses. In cases with gene rearrangements detected by FISH using only break-apart probes,Archer™ provided additional information on the partner fusion gene.
Conclusions: The Archer™ assay showed reproducible results that were concordant with those of conventional sarcoma oncogenic fusion gene detection methods,and has several advantages,including multiplexing capability,and detection of transcripts with heterogeneous fusion partners and variable breakpoints,as well as minor variant fusion transcripts,which may provide insight into tumor biology.

58 Recurrent Novel CIC Gene Abnormalities in Angiosarcoma: A Molecular Study of 120 Cases with Concurrent Investigation of PLCG1, KDR, MYC, and FLT4 Gene Alterations

Shih-Chiang Huang, Lei Zhang, Yun-Shao Sung, Yu-Chien Kao, Narasimhan P Agaram, Cristina Antonescu. Memorial Sloan Kettering Cancer Center, New York, NY; Chang Gung Memorial Hospital, Taoyuan City, Taiwan; Shuang Ho Hospital, Taipei Medical University, New Taipei City, Taiwan.
Background: Angiosarcoma (AS) is a rare sarcoma subtype showing considerable clinicopathologic and genetic heterogeneity. Most radiation-induced AS show *MYC* gene amplifications, with a subset of cases harboring *KDR*, *PTPRB* and *PLCG1* mutations. Despite these recent advances, the genetic abnormalities of most primary AS remain undefined.
Design: Whole transcriptome sequencing was initiated in 2 index cases of primary soft tissue AS with undifferentiated morphology occurring in young adults for novel gene discovery. The candidate abnormalities were validated and then screened by targeted sequencing and FISH in a large cohort of 120 well-characterized AS. Findings were subsequently correlated with the status of *KDR, PLCG1, MYC* and *FLT4* gene abnormalities. The clinicopathologic relevance and prognostic significance of these genetic changes were analyzed by statistical methods.
Results: Concurrent *CIC* mutations and *CIC* rearrangements were identified in both index cases, with a *CIC-LEUTX* fusion being detected in one. Upon screening, an additional visceral AS in a young adult had a complex *CIC* rearrangement, while 6 others harbored only *CIC* mutations. All 3 *CIC*-rearranged AS lacked vasoformation and had a solid growth of undifferentiated round to rhabdoid cells, showing immunoreactivity for CD31 and ERG and sharing a transcriptional signature with other round cell sarcomas, including *CIC*-rearranged tumors (upregulation of *ETV1, ETV4, ETV5*).
Conclusions: Overall, *CIC* abnormalities occurred in 9% (9/98) of cases tested, being related to primary AS, young age, and inferior disease-free survival. In contrast *PLCG1* and *KDR* mutations accounted for 9.5% and 7%, respectively, with a predilection for breast and bone/viscera location, regardless of *MYC* status. *MYC* amplification was present in most secondary AS related to breast cancer (91%) compared to other causes (25%) or primary AS (7%). *FLT4*-amplified AS lacked *PLCG1/KDR* mutations, occurring predominantly in *MYC*-amplified population, and showed poor prognosis. The divergent genetic abnormalities emerging in different AS subsets promise both challenges and opportunities in designing future clinical trials of targeted therapy in this disease.

59 Evaluation of NKX2-2 Expression in Round Cell Sarcomas Including Those with CIC-DUX4 and BCOR-CCNB3 Fusions and Tumors with EWSR1 Rearrangement: Relative Specificity for Ewing Sarcoma

Yin Hung, Christopher Fletcher, Jason L Hornick. Brigham and Women's Hospital, Boston, MA.
Background: Ewing sarcoma (ES), a round cell sarcoma predominantly arising in bone and soft tissue of children and adolescents, shows histologic overlap with other round cell tumors. About 90% of ES harbor *EWSR1-FLI1* gene rearrangement. NKX2-2, a homeodomain transcription factor involved in neuroendocrine/glial differentiation and a downstream target of *EWSR1-FLI1*, has been reported as an immunohistochemical (IHC) marker for ES. We assessed the specificity of NKX2-2 for ES compared to other ES-like sarcomas and its utility in other soft tissue tumors with *EWSR1* translocation.
Design: We evaluated whole-tissue sections from 270 cases: 40 ES (4 with atypical/large cell features), 20 *CIC-DUX4* sarcomas, 5 *BCOR-CCNB3* sarcomas, 9 unclassified round cell sarcomas, 10 poorly differentiated synovial sarcomas, 10 lymphoblastic lymphomas, 10 alveolar rhabdomyosarcomas, 10 embryonal rhabdomyosarcomas, 10 Merkel cell carcinomas, 10 small cell carcinomas, 20 melanomas, 5 NUT midline carcinomas, 10 Wilms tumors, 10 neuroblastomas, 10 olfactory neuroblastomas, 12 mesenchymal chondrosarcomas, 10 angiomatoid fibrous histiocytomas (AMFH), 10 clear cell sarcomas (CCS), 5 gastrointestinal neuroectodermal tumors (GNET), 5 desmoplastic small round cell tumors (DSRCT), 10 extraskeletal myxoid chondrosarcomas (EMCS), 10 myoepitheliomas, and 19 myoepithelial carcinomas. *EWSR1* rearrangements were confirmed in all ES (3 with *EWSR1-ERG* fusion), AMFH, GNET, and EMCS, and a subset of CCS and DSRCT. NKX2-2 positivity was defined as moderate to strong nuclear immunoreactivity in at least 5% of cells.
Results: NKX2-2 was positive in 37/40 (93%) ES, including all atypical ES and cases with known *EWSR1-FLI1* or *EWSR1-ERG* fusion; 85% of ES showed diffuse (>50%) staining. NKX2-2 was positive in 28/230 (12%) non-ES cases, including 9/12 (75%) mesenchymal chondrosarcomas, 8/10 (80%) olfactory neuroblastomas, 1 *CIC-DUX4* sarcoma, 1 poorly differentiated synovial sarcoma, 1 neuroblastoma, 2 unclassified round cell sarcomas, and 3 small cell carcinomas. All non-ES *EWSR1*-associated soft tissue tumors were negative for NKX2-2, apart from 1 DSRCT, 1 myoepithelioma, and 1 myoepithelial carcinoma.
Conclusions: As a sensitive and relatively specific IHC marker for ES, NKX2-2 may be helpful to distinguish ES from most histologic mimics including *CIC-DUX4* and *BCOR-CCNB3* sarcomas. Most other *EWSR1*-associated soft tissue tumors are also negative for NKX2.2.

60 Anchored Multiplexed PCR for Targeted Next Generation Sequencing Reveals Recurrent and Novel Gene Fusions in Aneurysmal Bone Cyst and No Fusion in Giant Cell Tumor of the Bone

Omar Jaber, Natalya Guseva, Aaron Stence, Benjamin Miller, Munir Tanas, Deqin Ma. University of Iowa, Iowa City, IA.
Background: Primary aneurysmal bone cyst (ABC) is now considered a neoplastic process due to recurrent translocations involving the USP6 gene at the short arm of chromosome 17 (17p13). By fluorescence in situ hybridization (FISH), up to 69% of primary ABCs were found to harbor USP6 translocations. No USP6 translocation was found in secondary ABC or other histological mimickers such as giant cell tumor (GCT) of the bone. The most common translocation in ABC, t(16;17)(q22;p13), fuses the oncogene USP6 next to a highly active CDH11 promoter to upregulate USP6 activity. Less common partners include TRAP150, ZNF9, OMD, and COL1A1. GCT can recur locally, metastasize to lung in some cases, and can rarely undergo malignant transformation. Differentiating primary ABC from its mimickers is important for treatment and prognosis. We evaluated 14 cases of ABC and 12 cases of GCT using a next generation sequencing (NGS)-based assay which allows simultaneous detection of multiple fusions and specific breakpoints at single-base resolution without prior knowledge of the partners.
Design: Fourteen ABCs (13 primary and 1 secondary) and 12 GCTs were identified from our archives. Total nucleic acid was extracted from formalin-fixed, paraffin-embedded (FFPE) tissue. Targeted RNA sequencing for gene fusions was performed using the Universal RNA Fusion Detection Kit (ArcherDX), the ArcherTM FusionPlexTM Sarcoma Panel and the Ion Torrent personal genomic machine (Life Technologies). Data were analyzed using the Archer Analysis Pipeline 3.3.
Results: USP6 gene fusions were identified in 9 of 13 primary ABCs (69%). CDH11-USP6, the most common fusion in ABC, was found in 5 cases. Two novel fusions were detected in 3 cases of ABCs; RUNX2-USP6 (2 cases; 1 case, tested twice) and PAFAH1B1-USP6 (1 case). No USP6 fusion product was found in the case of secondary ABC or the 12 GCT cases.
Conclusions: Recurrent USP6 fusions were detected in 69% of primary ABCs, similar to the detection rate by FISH. With this NGS-based method, we were able to discover two novel USP6 fusion partners (RUNX2 and PAFAH1B1), which are not amendable to detection by FISH. PAFAH1B1 mutation leads to lissencephaly associated with Miller-Dieker syndrome. RUNX2 is a key transcription factor associated with osteoblastic differentiation and skeletal morphogenesis. We are planning to perform further studies to understand the significance of RUNX2 in ABC pathogenesis.

61 Clinical and Pathological Correlation of ATRX Loss in Large Series of Leiomyosarcomas

Jolanta Jedrzkiewicz, Parnian Ahmadi, Davis Ingram, Vinod Ravi, Keila Torres, Andrew Futreal, Elizabeth G Demicco, Alexander Lazar, Wei-lien Wang. MD Anderson Cancer Center, Houston, TX; Mount Saini Hospital, New York, NY.

Background: Mutations in the α-thalassemia/mental retardation syndrome X-linked (*ATRX*) gene have been described in up to 30% of leiomyosarcomas. ATRX belongs to the family of chromatin remodeling proteins that assist in chromosomal segregation during mitosis, DNA methylation and developmental gene expression. We studied ATRX expression a large cohort of leiomyosarcomas, both soft tissue and uterine in origin, and examine for it clinical and pathological significance.

Design: 214 cases of leiomyosarcomas (LMS) were selected from our archives and compiled into a tissue microarray including: 46 primaries, 59 local recurrences and 109 distant metastases. Four-micron-thick sections were obtained and stained with commercially available ATRX antibody (Sigma-Aldrich, HPA001906; 1:2000). Intensity of nuclear staining (0-3) and proportion of tumor staining (0-100%) were assessed. Only cases with positive internal controls were considered for loss of expression. Clinical follow-up was obtained.

Results: The male to female ratio was 1:5. Follow-up time ranged between 3 and 50 months. Overall, 101 LMS (47%) showed loss of nuclear staining for ATRX. 17% of primary tumors had loss of ATRX compared to 45% of all advance disease ($p=0.00057$). More uterine primaries had loss of ATRX (52%) than soft tissue primaries (21%) ($p<0.0001$). ATRX was lost more in poorly differentiated tumors (53%) than moderately (39%) and well-differentiated ones (24%) ($p=0.0006$). The loss of ATRX correlated with earlier tumor recurrence ($p=0.06$), but not worse survival ($p=0.54$).

Conclusions: Loss of ATRX can be seen in a significant proportion of leiomyosarcomas with advanced disease, uterine origin and poor differentiation. Furthermore, loss of ATRX may portend a more aggressive local disease.

62 Epithelioid Schwannoma: Clinicopathologic Analysis of 63 Cases

Vickie Y Jo, Christopher Fletcher. Brigham and Women's Hospital & Harvard Medical School, Boston, MA.

Background: Epithelioid schwannoma is rare and may be difficult to recognize. Loss of SMARCB1/INI1 expression has been observed in a subset and rare cases of transformation to MPNST have been reported.

Design: 63 cases identified between 2002-2015 were retrieved from consultation files. H&E and immunohistochemical stains were examined. Clinical and follow-up data were obtained from referring pathologists.

Results: Patients were 30 men and 33 women; median age was 44 years (range 13-75). None had any known neurocristopathy. 3 patients were reported to have multiple lesions (2 each). Anatomic sites were upper limb (20), lower limb (13), trunk (13), shoulder/axilla (2), buttock (2), groin (1), scalp (1), GI (8), spinal cord (2), uterus (1). In somatic sites, 51 were dermal/subcutaneous and 1 subfascial. Tumor size range was 0.4-22.7 cm (median 1.2). Tumors were well-circumscribed with firm, lobular or cystic tan-yellow texture; 11 were associated with a nerve. Tumors showed multilobulated growth of uniform epithelioid cells in bundles and nests within a frequently myxoid or hyalinized stroma. Tumor cells had round nuclei and abundant palely eosinophilic cytoplasm, usually lacking significant pleomorphism or hyperchromasia. 28 cases had spindled foci resembling conventional schwannoma, 29 had areas resembling Antoni B or Verocay bodies and 14 had thick-walled hyaline vessels. 51/52 somatic tumors were encapsulated; all visceral tumors were unencapsulated. Other features included reticular/microcystic growth (4), cord-like growth (6), granular cell change (1). Mitoses numbered 0-9 per 10 HPF (median 1). None had necrosis. 23 had degenerative nuclear atypia. Focal striking cytologic atypia was present in 6 tumors (all encapsulated), 3 of which showed transformation to epithelioid MPNST. All tumors had diffuse S-100 positivity; INI1 was lost in 22/55. GFAP was positive (15/35). EMA was negative (0/51) but showed a perineurial capsule in 44 cases. Keratin was focal (2/38); melanocytic markers were negative. Most patients underwent excision (13 complete; 45 marginal/positive margins). Follow-up for 16 patients thus far (including 2 with cytologic atypia) show no recurrences.

Conclusions: Epithelioid schwannoma is a distinct variant, most commonly occurring in superficial soft tissue of limbs or trunk in adults. Tumors show diffuse S-100 positivity; 40% show INI1 loss. Based on preliminary data, epithelioid schwannoma has a generally benign clinical course, though malignant transformation is seen rarely. Some cases show notable cytologic atypia which may indicate a morphologic continuum with epithelioid MPNST.

63 Anastomosing Hemangiomas Arising in Unusual Locations: A Clinicopathological Study of 15 Cases Showing a Predilection for the Paraspinal Region

Ivy John, Andrew L Folpe. Mayo Clinic, Rochester, MN.

Background: Anastomosing hemangioma (AH), a recently recognized benign vascular neoplasm originally described in the kidney, may be confused with well-differentiated angiosarcoma, owing to its distinctive anastamosing, non-lobular pattern of growth, and the presence of mild endothelial cell nuclear atypia. Rare AH have been described in the liver and non-renal genitourinary sites. We report a series of 15 AH occurring in unusual locations, in particular the paravertebral soft tissues.

Design: All available slides from 15 cases of AH were retrieved from our archives and re-reviewed. Clinical, radiographical and follow-up information was obtained.

Results: Cases occurred in 9 M and 6 F (median 67 years of age; range 2 to 85 years). Eleven cases involved the soft tissues near the vertebral column, including cases described as para-vertebral (n=4), psoas (n=2), costovertebral angle (n=2), para-aortic, para-sacral, and retroperitoneum (n=1 each). Other locations included the anterior mediastinum, uterine cornu, infundibular pelvic ligament, and upper arm (n=1 each). Imaging studies, available in 13 cases, lacked characteristics sufficient for a diagnosis of hemangioma. The tumors ranged from 1.5 – 7.5 cm (median, 3.6 cm). All cases showed typical morphological features of AH, including a non-lobular, anastomosing proliferation of capillary-sized vessels with mild endothelial cell nuclear variablity, scattered" hobnail" endothelial cells, and small fibrin thrombi. Mitotic activity and necrosis were absent. Adipocytic metaplasia and extramedullary hematopoiesis were present in roughly 50% of cases. When performed, immunohistochemical studies showed expression of endothelial markers (e.g., CD31, CD34) and absent expression of other markers, including HHV8. Preliminary clinical follow-up has not revealed any local recurrences or metastases. In only one case did the submitting pathologist favor a diagnosis of AH; four cases were submitted specifically to exclude a well-differentiated angiosarcoma.

Conclusions: AH, originally described in the kidney, also seems to have a predilection for the soft tissues of the paraspinal region. In locations such as these, the diagnosis of AH may be particularly challenging, as imaging studies do not show classical features of hemangioma, and as tumors in these locations are often sampled with limited needle biopsies. Awareness of the distinctive morphological features of AH, and appreciation that AH may occur in non-genitourinary sites, should allow its confident distinction from potentially more aggressive lesions, in particular angiosarcoma.

64 Follicular Dendritic Cell Sarcomas: Insights into Its Molecular Landscape

George Jour, Ahmet Zehir, Mrinal M Gounder, Omar Abdel-Wahab, Jacklyn Casanova, Ahmet Dogan, Marc Ladanyi, David Klimstra, Maria E Arcila. Memorial Sloan Kettering Cancer Center, New York, NY; Memorial Sloan-Kettering Cancer Center, New York, NY.

Background: Follicular dendritic cell sarcoma (FDCS) is a rare mesenchymal neoplasm arising in intimate association with lymphoid tissue. It is highly heterogeneous, with a broad spectrum of presentations, pathologic phenotypes and clinical behavior. To date, the disease remains poorly understood at the clinical, pathologic and molecular levels. Herein, we investigate the molecular landscape of FDCS and seek candidate genes for targeted therapies.

Design: DNA from 18 FFPE tumors (16 patients) and matching normal tissue was extracted. Testing was performed by a laboratory developed custom hybridization-capture based assay (MSK-IMPACT) targeting all exons and selected introns of 410 key cancer genes. Barcoded libraries from tumor / normal pairs were captured and sequenced on an Illumina HiSeq 2500 and analyzed with a custom analysis pipeline.

Results: Our series includes 10 male and 6 female patients with a median age of 49 years (range 21-79). Anatomical sites included 4 retroperitoneal, 3 neck lymph nodes, 3 mediastinal, 3 tracheal, 2 liver, 1 colon, 1 chest wall, 1 axilla. A total of 52 mutations including 42 single nucleotide variants, 3 splice site variants, 1 nonsense mutation and 6 frameshift deletion. 2 cases showed no mutations or CNV. Cancer related pathways affected included: 1- Deleterious mutations in tumor suppressor genes *TP53,BAP1, PTEN, RB1, NF2, PTCH1 (7/18; 45%)* 2- Cell cycle check genes including *ATR, ATM, MDC1 (3/18;17 %).* 3- Chromatin remodeling and methylation/demethylation genes including *ARID1A, ARID1B, DNMT3A,B and DNMT1A (5/18;30%).* Amplification of *ETV6/CCND2* and *MDM2* was identified in 2 (10%) and 1 (5%) case, respectively. Comparison of primary and recurrent/metastatic tumors (2 patients) showed retention of baseline mutations with acquisition of additional alterations including *NOTCH1, ATR, NKX-2,* and *IGFR1.*

Conclusions: Genetic alterations in tumor suppressor genes rather than activation of oncogenes seem to drive tumorigenesis in FDCS. Loss of *PTCH1* and *MDM2* amplification in a small subset of cases identify possible candidates for targeted therapies with Smoothened (SMO) inhibitors and *MDM2* inhibitors . RNA sequencing and whole genome sequencing are warranted to identify potential undetected translocations.

65 Recurrent BCOR Internal Tandem Duplication (ITD) and YWHAE-NUTM2B Fusions in Undifferentiated Round Cell Sarcoma (URCS) of Infancy – Overlapping Genetic Features with Clear Cell Sarcoma of Kidney (CCSK)

Yu-Chien Kao, Shih-Chiang Huang, Pedram Argani, Catherine Chung, Nicole Graf, Rita Alaggio, Cristina Antonescu. Memorial Sloan Kettering Cancer Center, New York, NY; Shuang Ho Hospital, Taipei Medical University, Taipei, Taiwan; Chang Gung Memorial Hospital, Taoyuan, Taiwan; Johns Hopkins University School of Medicine, Baltimore, MD; The Hospital for Sick Children, Toronto, ON, Canada; The Children's Hospital of Westmead, Westmead, Australia; University of Padua, Padua, Italy.

Background: Infantile soft tissue URCS is a heterogeneous group of tumors, often lacking known genetic abnormalities. Based on a t(10;17;14) karyotype with similar breakpoints seen in CCSK (index case, pelvic, 4 month old boy) we have investigated the potential shared genetic abnormalities in CCSK and soft tissue URCS. CCSK are characterized either by *BCOR* exon 16 ITD in most cases or by *YWHAE-NUTM2B* fusions in 12% of cases.

Design: Among the 20 infantile URCS selected, 18 showed no known gene fusions, representing the study group. RNA sequencing was applied on 5 URCS with frozen tissue, the remaining being investigated for *YWHAE-NUTM2B* by FISH, and DNA PCR for *BCOR* ITD. A control group including: 3 CCSK, 6 fusion-negative URCS in older children or adults, and 5 cases of other types of infantile sarcomas, was tested for *BCOR* ITD and *YWHAE* abnormalities.

Results: The index case was validated for *YWHAE-NUTM2B* fusion by FISH and RT-PCR, while lacking *BCOR* ITD. A 2nd identical *YWHAE-NUTM2B* fusion was found in a back lesion from a 5 month old boy. The remaining 16 cases and control group lacked *YWHAE* gene rearrangements; instead *BCOR* ITD were found in 7/18 (39%) infantile URCS tested. In the control cohort, *BCOR* ITD was found only in the 3 CCSK, while

absent in all others. Histologically, URCS with both genotypes had similar appearance with CCSK, composed of uniform small blue round cells with fine chromatin, ocasional rosettes and prominent capillary network. The anatomic distribution included trunk (4), abdomen (3) and H&N (2). RNAseq showed BCOR overexpression in BCOR-ITD-positive cases compared to other URCS.
Conclusions: We report *BCOR* exon 16 ITD (39%) and *YWHAE-NUTM2B* fusions (12%) in infantile soft tissue URCS, but not in other subtypes or URCS of older children/adults. These findings suggest that a subset of infantile URCS show overlapping features with CCSK, such as age, histologic features and genetic signature. Based on this close pathogenetic link with CCSK, these URCS most likely represent the soft tissue counterparts of CCSK.

66 TLE1 mRNA Chromogenic In Situ Hybridization (CISH): A Potentially Powerful Diagnostic Tool for Synovial Sarcoma

Vadim Khachaturov, Rana Naous, Zhen Wang, John R Goldblum, Steven D Billings, Brian P Rubin. Cleveland Clinic, Cleveland, OH; SUNY Upstate Medical University, Syracuse, NY.
Background: Synovial sarcoma (SS) can be diagnosed by identifying its specific t(X;18) (*SS18-SSX1-2*) translocation with resultant *SS18-SSX* gene fusion by conventional cytogenetics, fluorescence in situ hybridization (FISH) or polymerase chain reaction (PCR). However, these methodologies are costly, labor intensive and aren't available in all institutions. *TLE1* was originally identified as strongly and differentially expressed in SS. Initial studies using TLE1 immunohistochemistry (IHC) as a surrogate were promising. However, due to technical issues, TLE1 IHC is no longer reliable. To better harness the potent discriminatory power of *TLE1* in the diagnosis of SS, we evaluated the utility of *TLE1* RNA CISH.
Design: We evaluated 40 cases for *TLE1* by mRNA CISH: SS (n=27; 19 MSS, 3 BSS, 5 PDSS), malignant peripheral nerve sheath tumor (MPNST) (n=7), dermatofibrosarcoma protuberans (DFSP) (n=4), and benign fibrous histiocytoma (BFH) (n=2). Twenty-one SS cases had confirmed *SS18* translocation. FFPE tissue sections were stained on Ventana Discovery XT automation system using *TLE1* and control probes from Advanced Cell Diagnostics (Heyward, CA). *TLE1* signal intensity was scored as strong, weak and negative, and the distribution was defined as diffuse (>50%), patchy (>25-50%), focal (5-25%) and negative (<5%).
Results: All SS cases were positive for *TLE1* RNA CISH while all cases of MPNST, DFSP & BFH were negative. Most SS exhibited strong and diffuse positivity, 81% and 70%, respectively. Rare focal (1/27, 4%) and weak (5/27, 19%) positivity were also observed. Variable heterogeneous *TLE1* expression was present in 56% of cases (15/27), more frequently in BSS (3/3, 100%) and PDSS (4/5, 80%) compared to MSS (8/19, 42%).

***TLE1* mRNA CISH Results**				
Diagnosis	**N**	**Strong**	**Weak**	**Neg.**
MSS	19	16/19	3/19	0/19
BSS	3	3/3	0/3	0/3
PDSS	5	3/5	2/5	0/5
Total SS	27	22/27	5/27	0/27
MPNST	7	0/7	0/7	7/7
DFSP	4	0/4	0/4	4/4
BFH	2	0/2	0/2	2/2

Conclusions: Preliminary results show *TLE1* RNA CISH to be a very useful diagnostic tool for SS with 100% sensitivity and specificity. The quick turnaround time and ease of interpretation with the ability to visualize the results by conventional light microscopy make RNA ISH comparable with IHC for ease of use. RNA CISH is a viable alternative for diagnostic markers where suitable commercial antibodies may not be available.

67 Spindle Cell/Pleomorphic Lipomas of the Distal Extremities: Not Just a Myth

Vadim Khachaturov, Jennifer S Ko, Jason L Hornick, John R Goldblum, Brian P Rubin, Steven D Billings. Cleveland Clinic, Cleveland, OH; Brigham and Women's Hospital, Boston, MA.
Background: Spindle cell/pleomorphic lipomas (SC/PLs) typically occur in older men and are often limited to the posterior neck/back area, including the shoulders. Cases outside this region, excluding dermal spindle cell lipomas, are exceedingly rare. We examined lesions classified as SC/PLs in men that arose in the distal extremities.
Design: Eight cases of histologically confirmed SC/PLs and located distally to the elbows and waist line were immunohistochemically evaluated for CD34, p16, Rb1, desmin and ER. Nuclear Rb1 staining was scored as retained (>75% +), mosaic (25-75% +) and lost (<25% +). Other markers were scored as diffuse (D+)(>50%), patchy (P+)(50 to 25%), focal (F+)(<25 to 5%) and negative (<5%).
Results: Patients ranged from 36 to 80 years of age (median 57) with a median tumor size of 5.1 cm. Most cases (6/8, 75%) were subfacial, 2 of which involved the subcutaneous tissue. The 2 exclusively subcutaneous cases were both from the thigh. Myxoid stroma was seen in 88% (7/8) of cases. One PL (#8) had plexiform vessels and multilocular lipoblasts. All cases were positive for CD34. Rb1 was lost in 88% (7/8) of cases; one case had a mosaic pattern of staining. P16 positivity was present in 75% of cases. All cases were negative for desmin and ER. Five of 5 cases tested were negative for MDM2 amplification. The remaining cases had follow-up data ranging from 122 to 158 months and none recurred.

Case	**Age/ Sex**	**Site/Size**	**Depth**	**Subtype**	**CD34/ Rb1**	**p16/Desmin/ ER**	**MDM2**
1	41/M	Popliteal/6.5 cm	Subfac.	SCL	F+/Lost	D+/Neg/Neg	UK
2	38/M	Knee/3.5 cm	Subfac.	SCL	D+/Lost	Neg/Neg/Neg	UK
3	36/M	Thigh/2.5 cm	Subcu.	SCL	D+/Lost	D+/Neg/Neg	UK
4	80/M	Thigh/11.2 cm	Subcu.	SCL	D+/Lost	P+/Neg/Neg	Namp
5	75/M	Forearm/20 cm	Subcu. to Subfac.	SCL	D+/ Mosaic	Neg/Neg/Neg	Namp
6	57/M	Foot/5.7 cm	Subcu. to Subfac.	PL	D+/Lost	D+/Neg/Neg	Namp
7	60/M	Hand/4.5 cm	Subfac.	PL	D+/Lost	D+/Neg/Neg	Namp
8	73/M	Forearm/4.3 cm	Subfac.	PL	D+/Lost	P+/Neg/Neg	Namp
UK, unknown; Namp, not amplified							

Conclusions: SC/PLs of the distal extremities share similar clinicopathological characteristics with cases from the posterior neck region, with the exception of being deeply seated. Diagnosis of SC/PLs of the extremities should be made cautiously and only after excluding atypical lipomatous tumor. P16 does not discriminate SC/PLs from ALTs.

68 Man Versus FISH: How Accurately Can Soft Tissue Experts Predict MDM2 Amplification of Deep Seated Adipocytic Neoplasms Based on Histology?

Vadim Khachaturov, John R Goldblum, Steven D Billings, Brian P Rubin. Cleveland Clinic, Cleveland, OH.
Background: Differentiating benign lipomatous tumors (BLT) (lipomas, hibernomas, etc) from atypical lipomatous tumors/well-differentiated liposarcomas (ALT/WDLPS) has become substantially easier with the aid of *MDM2* fluorescence in situ hybridization (FISH) to detect *MDM2* gene amplification, the defining molecular signature of ALT/WDLPS. In this study, we sought to determine in a subspecialty consultation setting whether histology was sufficient to accurately diagnose ALT/WDLPS without the need to test for *MDM2* amplification.
Design: Three soft tissue pathologists (SDB, JRG & BPR) and their fellow (VK) evaluated deep seated adipocytic neoplasms prospectively using only hematoxylin and eosin stained sides and a diagnosis was rendered. All cases were subsequently tested for *MDM2* gene amplification by FISH. Clinical parameters, including age, sex, site and size were made available to each reviewer. Histological features used to diagnose ALT/WDLPS were variation in adipocyte size, hyperchromatic adipocytic nuclei, and cellular fibrous areas and blood vessel walls with atypical spindled stromal cells.
Results: There were 19 cases; 8 ALT/WDLPS in 5 men and 3 women ranging from 38 to 90 years of age (median 65) with a median tumor size of 19 cm, and 11 benign adipocytic tumors in 5 men and 6 women ranging from 40 to 78 years of age (median 48) with a median tumor size of 7.5 cm. Most of the retroperitoneal tumors were ALT/WDLPS (75%, 3/4) compared to 36% (5/14) from the extremities. The majority of BLTs consisted of lipomas with fat necrosis (7/11, 64%) followed by intramuscular lipomas (2), a lipoma and a hibernoma. On average, attending pathologists had a 93% accuracy rate of predicating *MDM2* amplification; they were more likely to over call (16%) than undercall (5%) ALT/WDLPS. The fellow had an 84% accuracy rate with more undercalling than overcalling, 11% and 5%, respectively. A total of 4 cases, 2 ALT/WDLPS and 2 lipomas were incorrectly interpreted, all of which had significant fat necrosis; one of the cases was an endobronchial lipoma with extensive fibrosis.
Conclusions: Even in the hands of expert soft tissue pathologists, histology comes close to but does not match the accuracy of *MDM2* gene amplification. Fat necrosis is the main culprit for human errors, which can be seen in both ALT/WDLPS and BLTs and often led to overcalling lipomas as ALT/WDLPS. For the time being, it appears that it is still necessary to test most, if not all deep-seated adipocytic tumors with *MDM2* FISH.

69 RNA-seq Study of TFE3 Translocation-Associated Perivascular Epithelioid Cell Neoplasm (PEComa)

Pallavi Khattar, Weihua Huang, Ximing Yang, Patricia V Adem, John T Fallon, Minghao Zhong. Westchester Medical Center at New York Medical College, Valhalla, NY; NorthWestern University Feinberg School of Medicine, Chicago, IL.
Background: Perivascular epithelioid cell neoplasms (PEComa) are a family of rare mesenchymal tumors with unknown cell origin. Several studies have reported small portion of those cases associated with *TFE3* rearrangement. Previously, we successfully identified *TFE3* fusion by RNA-seq from formalin fixed paraffin embedded (FFPE) tissue. Here, we would like to apply this massively parallel sequencing technology to study *TFE3* translocation-associated PEComa.
Design: 4 cases of *TFE3* translocation-associated PEComa (confirmed by FISH) were collected for RNA-seq. Total RNA was extracted from FFPE tissue, using the AllPrep DNA/RNA FFPE. 100 ng RNA was applied for sequencing library preparation using the TruSeq RNA Access Library Prep Kit as per the manufacturer's protocol. Paired-end sequencing (75 bp×2) was performed using the MiSeq Reagent V3 Kit (150 cycles) and the MiSeq sequencing system. STAR algorithm was employed for detection of any potential *TFE3* or other fusions. Bowtie2 was employed for alignment and mapping of short sequence reads to the human genome reference hg19 and the fusion transcript *SFPQ/PSF-TFE3*. Integrative Genomics Viewer (IGV) was employed for data visualization.
Results: We identified 3 cases with *PSF-TFE3* fusion, one case with *FOXO1-MTFP1* fusion.

Conclusions: It is feasible to perform RNA-seq for gene fusion from FFPE tissue. We confirmed the presence of *PSF-TFE3* fusion in small portion of PEComa cases. PEComa may carry other gene fusion, such as: *FOXO1-MTFP1*.

70 SWI/SNF Chromatin Remodeling Complex Status in SMARCB1/INI1-Preserved Epithelioid Sarcoma Cases

Kenichi Kohashi, Hidetaka Yamamoto, Yuichi Yamada, Yoshinao Oda. Department of Anatomic Pathology, Graduate School of Medical Sciences, Kyushu University, Fukuoka, Japan.

Background: SWI/SNF chromatin remodeling complex utilizes the energy of ATP hybrolysis to remodel nucleosomes and to modulate transcription. This complex is composed of evolutionarily conserved core subunits: SMARCB1 (INI1), SMARCA4 (BRG1), SMARCC1 (BAF155) and SMARCA2 (BAF170). Epithelioid sarcoma and malignant rhabdoid tumor which classified as tumor of uncertain differentiation almost show a complete loss of INI1 protein expression. However, a few cases of epithelioid sarcoma preserve INI1 protein expression, and clinicopathological features of these cases are uncertain. Meanwhile, INI1-preserved malignant rhabdoid tumor case identified as loss of BRG1 expression has been reported. To date, there has been no investigation focused on SWI/SNF chromatin remodeling complex in INI1-preserved epithelioid sarcoma cases.

Design: A check of INI1 immunoexpression status in 61 formalin-fixed paraffin-embedded epithelioid sarcoma specimens (proximal-type, 29 cases; conventional-type, 32 cases) was firstly performed. In available INI1-preserved epithelioid sarcoma cases, we analyzed the BRG1, BAF155 and BAF170 protein expression. As for these proteins, immunoreactivities were classified into two categories: -, no staining of tumor nuclei; +, any nuclear staining above background.

Results: INI1-preservation was observed in 6 of 29 (21%) proximal-type and 3 of 32 (9%) conventional-type epithelioid sarcoma cases. Seven cases of INI1-preserved epithelioid sarcoma (6 proximal-type and 1 conventional-type) were available for further immunohistochemical study. Each one case of proximal-type and conventional-type showed loss of BAF170, and 2 proximal-type cases revealed loss of BRG1, but the other remaining core subunit proteins were preserved. One proximal-type case disclosed mosaic pattern of BRG1 and loss of BAF155. However, in remaining 2 proximal-type cases, all core subunit proteins were preserved.

Conclusions: Five of the 7 cases of INI1-preserved epithelioid sarcoma show loss of one or more SWI/SNF chromatin remodeling core subunit proteins. Our findings may support a role of SWI/SNF chromatin remodeling complex in the tumorigenesis of INI1-preserved epithelioid sarcoma cases.

71 Utility of a Pan Genomic Fusion Panel (1300 Genes) on a Next Generation Sequencing (NGS) Platform in Evaluation of Bone and Soft Tissue Sarcoma

Ravindra Kolhe, Karen Fritchie, Alka Chaubey, Lisa C Watson, Claire Attwooll, WonSok Lee, Deepa Jagdale, Ashis K Mondal. Georgia Regents University, Augusta, GA; Mayo Clinic, Rochester, MN; Illumina, Inc, San Diego, CA; Greenwood Genetic Center, Greenwood, SC.

Background: Identification of novel gene fusions in sarcomas can provide substantial tumor-specific information for research, & shows potential for diagnostic and targeted treatment purposes. Even though florescence in situ hybridization (FISH) is the current gold standard in fusion detection, it is limited in the number of genes it can detect in parallel. Similarly qPCR technique is restricted by the same limitation & both lack high-resolution molecular characterization which is crucial for understanding the identity of these fusion partners. In contrast, RNA sequencing (RNA-Seq) is a powerful approach for simultaneous discovery of all possible fusion junctions in a single reaction. As oncogenes can fuse to multiple partners, the major advantage of using RNA-Seq technology is the ability to accurately identify fusions of all genes in the panel in a single sequencing assay, even without prior knowledge of fusion partners or breakpoints. In the current study, we assess the potential of an RNA-Seq capture panel consisting of 1300 fusion and cancer-associated genes, for identifying new gene fusions in sarcoma.

Design: Archived Sarcoma cases (Fig.1) were retrieved & the diagnoses was confirmed. Subsequently, RNA sequencing was performed on RNA isolated from FFPE blocks on a NGS platform (MiSeq, Illumina). The fusion calls were read & interpreted on the software provided by the manufacture. The results were compared with conventional FISH studies & karyotyping.

Results: The fusion calls with high confidence on the NGS platform matched 100% with the FISH findings/karyotype on all the cases.

No.	Chr1	Pos1	Chr2	Pos2	Depth	Fusion Reads	Gene1	Gene2	Histological Diagnosis	FISH /Karyotype Findings	Histology/FISH/NGS correlation
1	chr22	29683123	chr11	128651853	581	19	EWSR1	FLI1	Ewing Sarcoma	Karyo: t(12;22)(q13.3; q12) FISH: EWSR1 (22q12) translocation identified.	100% Match
2	chr22	29683123	chr11	128651853	783	35	EWSR1	FLI1	Ewing Sarcoma	Karyo: t(12;22)(q13.3; q12) FISH: EWSR1 (22q12) translocation identified	100% Match
3	chr15	57384088	chr9	102590322	1495	242	TCF12	NR4A3	Extraskeletal myxoid chondrosarcoma	FISH: NR4A3 rearrangement was identified and EWSR1 rearrangement was not identified.	100% Match

Table 1: Summary of findings. RNA seq confirmed all the FISH findings in our 3 cases. In EMC by dual-color break-apart probe (FISH) we identified rearrangement in NR4A3 and there was no evidence of a EWSR1 rearrangement. By RNA seq not only we could confirm the rearrangement of NR4A3, but also identify its fusion partner (TCF12), which is reported in minority of EMC cases.

Conclusions: Here for the first time we describe an approach for selective enrichment of cancer-associated genes from RNA-Seq libraries that requires only a fraction of the sequencing depth and enables simultaneous fusion detection and expression profiling of over 1300 cancer-associated genes in one assay. We anticipate that this approach of obtaining high-resolution RNA-Seq data from an FFPE sample at reduced sequencing cost, will facilitate studies of sarcomas that were not previously possible.

72 Chondroblastoma of Extracranofacial Bones - Analyses of 103 Cases by Numerical Scoring on Histology

Eiichi Konishi, Yasuaki Nakashima, Masayuki Mano, Yasuhiko Tomita, Sanae Yamazaki, Akio Yanagisawa. Kyoto Prefectural University of Medicine, Kyoto, Japan; Kyoto University, Kyoto, Japan; Osaka National Hospital, Osaka, Japan; Osaka Medical Center of Cancer and Cardiovascular Diseases, Osaka, Japan.

Background: Chondroblastoma (CB) is a rare chondrogenic tumor and categorized as a locally aggressive, rarely metastasizing intermediate bone tumor. No reliable clinicopathologic parameters predicting the local recurrence and/or very rare pulmonary metastasis, however, have been elucidated.

Design: Clinicopathological profiles of 103 cases of histologically proven CB of extracraniofacial bones were retrieved. Radiological images and pathological slides were reviewed. For each case, 10 pathological and 5 radiological features were evaluated by numerical scoring and were analyzed statistically in terms of prognostic significance.

Results: Of 103 cases, age of the patients was ranged 8-61 (average: 19.6 years) with 80 male and 23 female. Frequently involved sites were femur (43.7%), tibia (14.6%), calcaneus (12.6%), patella and humerus (9.7%). Radiologically, tumor were 2-80 (average: 31.1) mm in size, with marginal sclerosis (94.3%) and calcification (55.9%). Histologically, there were immature pink cartilage (91.4%), mitotic figures (44.1%), and chicken wire calcification (32.3%). Curettage was usually selected for the initial surgery (91.2%). For the follow-up period ranging 2-260 (average: 53.5) months, local recurrence was noted in 16 cases (15.5%), with period since the initial surgery till the recurrence ranging 4-53 (average: 20.2) months. No patient had metastasis. Recurrent sites were femur (37.5%), tibia (25.0%), humerus (18.8%), patella, and calcaneus (6.25%). By univariate analysis, only cystic change in radiological image was statistically significant for differentiating recurrent cases from non-recurrent cases. Age of the patients with recurrence was statistically younger than that of the patients without recurrence. Other features, such as sex, tumor size, location, mitotic figures, surgical methods, etc. were insignificant. In multivariate analysis, we could not find any features which predict local recurrence.

Conclusions: In this study, we could not find the clinicopathological features predicting the local recurrence. Local recurrence rate was similar to the previous reports (5-20%), but metastasizing case was not noted. CB is categorized into "rarely metastasizing tumor" which can metastasize in less than "2%", but the current date shows metastasis of extracraniofacial CB is extremely rare.

73 ETV4 Is a Useful Marker for the Diagnosis of CIC-DUX4 Round Cell Sarcomas: A Study of 110 Cases Including Mimicking Lesions

Sophie Le Guellec, Valerie Velasco, Gaelle Perot, Sarah Watson, Franck Tirode, Jean-Michel Coindre. Institut Claudius Regaud, Toulouse, France; Institut Bergonié, Bordeaux, France; Institut Curie, Paris, France.

Background: A subset of primitive round cell sarcomas (RCS) remains difficult to diagnose and classify. Among these, a rare RCS harboring a novel gene fusion, *CIC-DUX4*, has been described. Due to its aggressive clinical behavior and potential therapeutic implications, accurate identification of this novel soft tissue sarcoma is necessary. Definitive diagnosis requires molecular confirmation but yet only few centers can perform this test. Based on several studies that *CIC-DUX4* RCS show upregulation of *PEA3* subfamily genes (belonging to *ETS* transcription factors family) and notably *ETV4*, we performed a detailed immunohistochemical analysis to investigate the expression of ETV4 among *CIC-DUX4* RCS and their potential mimics (especially Ewing sarcomas).

Design: The study cohort included 15 cases of *CIC-DUX4* RCS and 95 tumors that could mimic *CIC-DUX4* RCS morphologically: 40 Ewing sarcomas (*EWSR1* rearrangement detected by Fluorescent In Situ Hybridization (FISH)), 25 alveolar rhabdomyosarcoma (*FKHR* rearrangement detected by FISH), 20 poor differentiated, round cell synovial sarcoma (*SS18* rearrangement detected by FISH) and 10 desmoplastic round cell tumors (*WT1-EWSR1* detected by Reverse-Transcriptase Polymerase Chain Reaction (RT-PCR)).

Results: All *CIC-DUX4* RCS (on core needle biopsies and open biopsies) showed strong and diffuse ETV4 nuclear positivity.

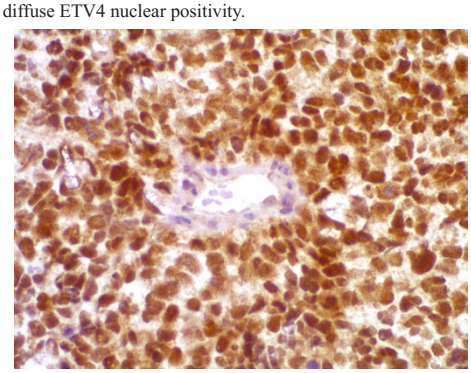

Among other 95 tumors, only six cases (4 Ewing sarcoma, one alveolar rhabdomyosarcoma and one desmoplastic round cell tumors) showed focal (<5% of tumors cells) and very weak nuclear expression of ETV4; and all other tumors (on core needle biopsies and open biopsies) were completely negative for ETV4.

Conclusions: ETV4 is a useful diagnostic marker in *CIC-DUX4* round cells sarcoma. Faced with histologic diagnosis of round cell undifferentiated soft tissue sarcomas that lack molecular evidence of a known sarcoma-associated translocation, a systematic

immunohistochemical evaluation of ETV4, even on core needle biopsies, allows a valuable selection of cases for FISH analysis permitting the definitive diagnosis of *CIC-DUX4* sarcomas.

74 Malignant Peripheral Nerve Sheath Tumor Is a Challenging Diagnosis: A Systematic Pathology Review, Immunohistochemistery and Molecular Analysis in 160 Patients from the French Sarcoma Group Database

Sophie Le Guellec, Anne-Valerie Decouvelaere, Thomas Filleron, Isabelle Valo, Celine Charon-Barra, Yves-Marie Robin, Philippe Terrier, Christine Chevreau, Jean-Michel Coindre. Institut Claudius Regaud, Toulouse, France; Centre Léon Bérard, Lyon, France; Centre Paul Papin, Angers, France; Centre Georges-François Leclerc, Dijon, France; Centre Oscar Lambret, Lille, France; Institut Gustave Roussy, Paris, France; Institut Bergonié, Bordeaux, France.

Background: An accurate histopathologic diagnosis is essential for an adequate treatment of soft tissue sarcomas. The diagnosis of malignant peripheral nerve sheath tumor (MPNST) can be complex, particularly outside the neurofibromatosis type 1 (NF1) context. MPNST is a rare malignancy and due to the lack of specific histological criteria, a number of non-MPNSTs were placed incorrectly in this category over the years and prognostic factors remain controversial.

Design: Three hundred and fifty patients diagnosed with MPNST (from 1990 to 2013) were retrieved from the French sarcoma network (http://www.rreps.sarcomabcb.org) and the Conticabase (http://www.conticabase.sarcomabcb.org). Tumor samples were available for 160 cases (45.2%). Pathology review, immunohistochemistry and molecular analysis (when dealing with a monomorphic sarcoma suspected of showing simple genomic alteration) were systematically performed. Patient, tumor, and treatment characteristics were evaluated to identify prognostic factors for the undeniable primary MPNST (n=106) cohort.

Results: Twenty-nine tumors (18.1%) initially diagnosed as MPNST were reclassified. Patients with NF1 disease comprised 64% of the remaining cohort. The 5-year overall survival for patients from the entire cohort was 46.96%, 34.78% for NF1 patients and 68.54% for patients without NF1 disease, making NF1 syndrome an independent poor prognostic factor of survival. Positive margins and lack of radiation therapy were independent predictors of local recurrence. Tumor grade (FNCLCC (Fédération Nationale des Centres de Lutte Contre le Cancer) grading system) was an independent prognostic indicator of metastasis.

Conclusions: Given the therapeutic implications of a misdiagnosis, the systematic pathology review, immunohistochemistry and molecular analysis (when dealing with monomorphic sarcoma) strategy allowed reclassification of 20% of cases, mainly in the sporadic MPNSTs. We, therefore, propose it as a standard management procedure for all sarcomas. Patients with MPNSTs shared prognostic factors similar to those observed in patients with other soft tissue sarcomas. A deeper understanding of NF1 associated-MPNST is needed to allow the identification of new treatment strategies.

75 Transcriptomic Reappraisal Identifies Overexpressed PLCB4 as an Adverse Prognosticator in Primary Localized Gastrointestinal Stromal Tumors (GISTs)

Chien-Feng Li, I-Chieh Chuang, Hsuan-Ying Huang. Chi Mei Medical Center, Tainan, Taiwan; Kaohsiung Chang Gung Memorial Hospital and Chang Gung University College of Medicine, Kaohsiung, Taiwan.

Background: In the post-imatinib era, accurate prognostication of GISTs is a critical issue for both outcomes counseling and identifying other targetable molecules because of inevitable imatinib resistance. Despite being a cancer hallmark of renewed interest, deregulated cellular metabolism remains barely elucidated in GISTs, especially in the arena of lipid bioprocessing.

Design: Through data mining of published transcriptomes (GSE8167), we sought for lipid catabolism-regulating metabolic drivers differentially upregulated in high-risk cases and identified *PLCB4* (phospholipase C; beta 4) as a top-ranking candidate relevant to GIST progression. PLCB4 expression status was validated in 3 GIST cell lines and two independent cohorts of formalin-fixed primary localized GISTs. Of these, *PLCB4* mRNA abundance measured by Quantigene assay was informative in 70 cases, and immunoexpression level informative by H-score method in another 350 cases on tissue microarrays, including 213 cases with known *KIT/PDGFRA* mutation genotypes. The obtained data were correlated with clincopathological and *KIT/PDGFRA* genotypic variables and disease-free survival (DFS).

Results: Both imatinib-sensitive GIST882 cells and imatinib-resistant GIST48 cells exhibited increased expression of *PLCB4* mRNA and protein, compared with no expression detectable in imatinib-resistant GIST430 cells. PLCB4 mRNA expression significantly increased from adjacent normal tissue to the non-high-risk group ($p=0.007$) and from non-high-risk group to high-risk GISTs ($p=0.008$). PLCB4 protein overexpression was associated with non-gastric location ($p=0.022$), unfavorable genotypes ($p=0.033$) and strongly related to increased size, mitosis, and risk level defined by both NIH and NCCN schemes (all $p<0.001$). Univariately, decreased DFS was strongly associated with PCLB4 overexpression ($p<0.0001$), which remained prognostically independent to predict adverse outcome ($p<0.001$, hazard ratio: 3.075), together with epithelioid histology and higher risk levels.

Conclusions: PLCB4is a novel lipid catabolism-regulating enzyme closely linked to GIST progression, given its strong associations with unfavorable clincopathological and genotypic factors and independent negative prognostic impact.

76 BCOR-CCNB3 Sarcoma of Soft Tissue with Round and Spindle Histology: A Study of 4 Cases Highlights the Pitfall of Mimicking Poorly Differentiated Synovial Sarcoma

I-Chuang Liao, Wan-Shan Li, Hsuan-Ying Huang. National Cheng Kung University Hospital, Tainan, Taiwan; E-Da Hospital, Kaohsiung, Taiwan; Kaohsiung Chang Gung Memorial Hospital, Kaohsiung, Taiwan.

Background: Derived from X-chromosome paracentric inversion, *BCOR-CCNB3* fusion is the molecular hallmark of a recently described undifferentiated sarcoma, predominantly occurring in the bones of male adolescents and exhibiting "Ewing-like" round cells. Only 13 molecularly validated cases were reported to primarily originate in the soft tissue, leaving the histological spectrum and tumor behavior largely undefined.

Design: Four undifferentiated sarcomas of soft tissue comprising round and spindle cells were identified from archives. Despite being variably reactive to synovial sarcoma (SS)-related markers, these cases were excluded by negative SS18-SSX/RT-PCR and/or SYT/FISH assays, further stained with cyclinB3, and confirmed by RT-PCR to harbor *BCOR-CCNB3* transcript using formalin-fixed tissue. The clinicopathological features and treatment outcomes were analyzed.

Results: Including 2 teenagers (14 y, 17y) and 2 middle-aged adults (34y, 44y), four male patients had deep-seated intramuscular tumors in the buttock, pelvis, back, and thigh, respectively, the mean size of which was 10.7 cm (range, 7-14). Histologically, solid sheets of primitive round to ovoid cells constitute the major component with vesicular nuclei and fine chromatin, a median mitotic count of 36 (range, 28-41) per 10 HPFs, and focal geographic necrosis and staghorn vasculature. From 10% to 40%, fascicular growth of spindle cells was distinctive in all cases, with 1 being reactive to EMA, 2 to TLE1, and 4 to CD99 (patchy in 3; diffuse in 1), hence reminiscent of poorly differentiated SS. Notably, all cases showed strong nuclear cyclinB3 staining and *BCOR-CCNB3* fusion by RT-PCR with confirmatory sequencing. At last follow-up (median, 9.3 m), one patient developing lung metastasis at 15 m was dead of disease at 20 m postoperatively, one free of disease, and two alive with tumors.

Conclusions: *BCOR-CCNB3* sarcoma is clinically aggressive mesenchymal malignancy with a predilection for males. However, it may primarily arise from soft tissue, occur in adults, and display SS-mimicking round and spindle cell histology. CyclinB3 is a useful screen tool to select candidate cases for *BCOR-CCNB3* molecular testing.

77 Superficial Angiomyxoma Is Characterized by Loss of PRKAR1A Expression

Adrian Marino-Enriquez, Christopher Fletcher, Leona A Doyle. Department of Pathology, Brigham and Women's Hospital and Harvard Medical School, Boston, MA.

Background: Superficial angiomyxoma (SAM) is a rare subcutaneous neoplasm that occurs sporadically or, much less frequently, in the context of Carney complex, an autosomal dominant multiple neoplasia syndrome caused by germline *PRKAR1A* inactivating mutations. There are no diagnostic markers for SAM and its genetics are poorly understood. The purpose of this study was to evaluate the expression of PRKAR1A in SAM by immunohistochemistry, and to correlate the findings with *PRKAR1A* mutational status.

Design: 32 cases were retrieved and the diagnosis of SAM was confirmed on H&E. Patients included 14 females and 18 males (age range 3-74, median 42), 5 of whom were suspected to be affected by Carney complex. PRKAR1A protein expression was evaluated by immunohistochemistry, using a monoclonal antibody to the RI-alpha subunit (Origene, Clone 6C7, 1:6500); expression was considered lost when neoplastic cells lacked staining in the presence of cytoplasmic reactivity in non-neoplastic cells, which served as internal controls. DNA was extracted from formalin-fixed paraffin-embedded tissue sections from 4 cases and analyzed by targeted exon hybrid-capture and high-throughput sequencing on the Oncopanel platform (interrogating exonic sequences of 300 cancer-associated genes, including *PRKAR1A*, as well as 113 introns across 35 genes). *PRKAR1A* sequences were manually reviewed using IGV (Integrative Genomics Viewer).

Results: Histologically, cases of SAM were typically multilobulated and composed of a paucicellular proliferation of bland spindle cells with scant cytoplasm, set in an abundant myxoid matrix with thin-walled vessels and scattered inflammatory cells, predominantly neutrophils. 21 cases (66%) showed complete loss of PRKAR1A expression in neoplastic cells, including 4 (of 5) cases with suspicion for Carney complex; the remaining 10 cases retained cytoplasmic expression. 2 (of 2) cases with loss of PRKAR1A by immunohistochemistry showed inactivating mutations of *PRKAR1A* (a c.569TGG>TAG (p.W190*) truncating mutation, and a c.489_490delTG frameshift mutation). 2 (of 2) PRKAR1A-positive cases, showed wild-type PRKAR1A sequence. No other recurrent mutations or copy number alterations were detected.

Conclusions: The majority of SAM (66%) show loss of PRKAR1A expression, providing a potential diagnostic marker and underscoring the critical role of PRKAR1A in the pathogenesis of SAM. *PRKAR1A* loss-of-function mutations can be identified by high-throughput sequencing in SAM, and correlate with loss of PRKAR1A protein expression by immunohistochemistry.

78 Programmed Death-Ligand 1 Expression in Sarcomas, a Clinical a Pathologic Study

Stemm Matthew, Alexander C Mackinnon. Medical College of Wisconsin, Milwaukee, WI.

Background: The interaction of programmed death-ligand 1 (PD-L1) and its associated receptor PD-1 is known to cause an inhibitory signal to the host immune response. This process has been exploited by tumor cells and overexpression of PD-L1 has been shown in some cancers to be an independent predictor of prognosis as well as a potential target for new therapies. The expression and prognosis of PD-L1 and PD-1 on sarcomas is unknown and warrants investigation as current treatment options for many sarcomas are limited and often ineffective.

Design: Sarcomas cases included in the radiation oncology database of this institution over the past 15 years were reviewed for this study. Cases with a treatment naïve biopsy and/or adjuvant-treated resection specimen were included. Eighty-five patients met criteria and were used to create multiple tissue microarrays. Two PD-L1 clones (Cell Signaling, E1L3N; Spring BioScience, SP142) and 1 PD-1 clone (Abcam, NAT105; Biocare, NAT105) were optimized for this study. Cases were considered positive for each clone if greater than 5% staining was detected.
Results: Most cases had both a pre-treatment biopsy and post-treatment resection for analysis. The tumors showed similar staining across all clones. Seventeen out of 85 tumors were considered positive including 5 out of 11 myxofibrosarcomas, 4 out of 19 high-grade undifferentiated pleomorphic sarcomas, 2 out of 6 leiomyosarcomas, 1 out of 6 dedifferentiated liposarcomas, 1 out of 1 rhabdomyosarcoma, 1 out of 2 malignant solitary fibrous tumors, 1 out of 5 malignant peripheral nerve sheath tumors, 1 out of 8 myxoid liposarcomas, and 1 out of 10 synovial sarcomas. Other tumors (17) such as well-differentiated liposarcomas, epithelioid sarcomas, and other miscellaneous sarcomas were negative. Four out of the 20 patients that showed extensive tumor necrosis in response to radiation were positive for PD-L1 overexpression. Five out of the 8 positive cases with a paired pre-treatment biopsy and post-treatment resection showed gain of PD-L1 expression following therapy.
Conclusions: PD-L1 or PD-1 overexpression is seen in a variety of sarcomas. Based on these results, staining with PD-L1 may be used to include patients in future clinical trials for anti-PD-L1 therapy. Tumors that showed strong response to radiation therapy showed greater than expected PD-L1 staining. In other tumors, PD-L1 overexpression may be a mechanism by which tumor cells continue to survive following radiation therapy.

79 The Wnt Signaling Antagonist Sclerostin in Osteosarcoma

Carolyn A Meyers, Jia Shen, Swati Shrestha, Greg Asatrian, Gregory LaChaud, Vi Nguyen, Arun Singh, Noah Federman, Sarah M Dry, Kang Ting, Chia Soo, Aaron James. University of California, Los Angeles, Los Angeles, CA.
Background: Sclerostin (SOST) is a Wnt signaling antagonist with high endogenous expression in osteocytes. SOST negatively regulates bone mass, and significant interests exist in the use of anti-SOST neutralizing antibodies for osteoporosis (currently in Phase III clinical trials). Despite this, the expression and function of SOST in osteosarcoma is entirely unknown.
Design: The relative expression of *SOST* was examined across seven osteosarcoma (OS) cell lines by quantitative RT-PCR, with or without osteogenic conditions. Next, immunohistochemical detection of SOST was performed in a wide array of human OS tumors and OS subtypes (n=41 tumors). Semi-quantification of immunostaining intensity, distribution was performed, including spatial correlation with bone matrix production and osteogenic markers expression.
Results: *SOST* expression varied widely between OS cell lines, with >97 fold variation. However, *SOST* expression significantly increased with osteogenic differentiation in all neoplastic cells in a time dependent fashion (**Fig. 1A**, KHOS312H shown). Immunohistochemical detection of SOST was present in the majority of OS specimens (87.8%, 36/41). Although variable, in general SOST immunoreactivity was observed in a large minority of OS tumor cells in a given biopsy specimen (mean: 42.4% of cells stained, SD: 31%). SOST expression was highly correlated with the presence and degree of neoplastic osteoid (**Fig. 1B**, lung metastasis of osteoblastic OS shown, $^{**}P<0.01$). This spatial correlation was confirmed via co-expression of SOST with traditional markers of osteodifferentiation, including BSP and OCN.

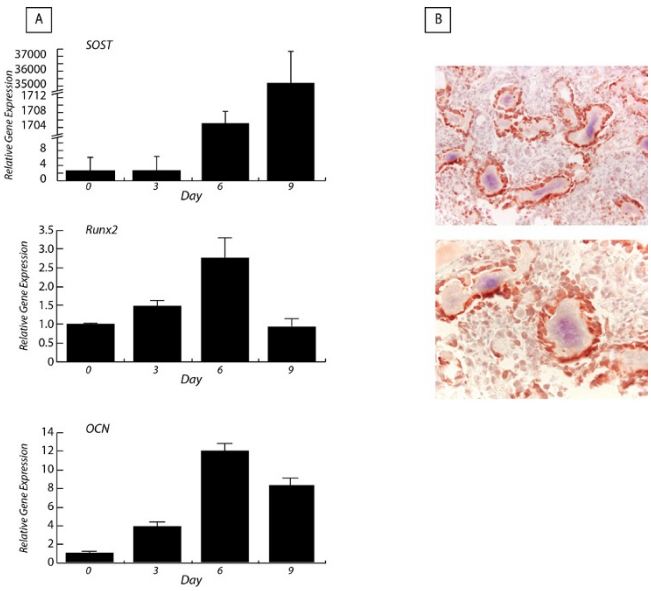

Conclusions: Sclerostin is frequently expressed in OS cell lines and tumor samples. Both the spatial correlation with osteoid and the *in vitro* expression patterns are in line with the known functions of SOST in non-neoplastic bone. In aggregate, these findings suggest that SOST may have a similar biologic function in OS, as a feedback inhibitor on osteogenic differentiation. Ongoing areas of investigation include the effects of forced *SOST* overexpression on OS cell proliferation, differentiation, and sensitivity to chemotherapy. Although anti-SOST therapies for osteoporosis may become a clinical reality in the near future, their basic biologic and phenotypic consequences in bone tumors should not be overlooked.

80 Diagnostic Value of Histone 3 Mutations in Osteoclast-Rich Bone Tumors

Erik Nohr, Marco Perizzolo, Lik Hang Lee, Justin M Cates, Doug Demetrick, Doha Itani. University of Calgary / Calgary Laboratory Services, Calgary, AB, Canada; Vanderbilt University Medical Center, Nashville, TN.
Background: Differentiating osteoclast-rich lesions of bone (giant cell tumor of bone (GCTB), chondroblastoma (CBA) and aneurysmal bone cyst (ABC)) may be challenging, especially on small biopsies. Recently, genetic aberrations in GCTB and CBA have been defined. G34W alteration of *H3F3A* is often seen in GCTBs and K36M mutation of both *H3F3A* and *H3F3B* are present in many CBAs. We aim to devise a simple assay to capture these mutations.
Design: Tissue from 117 curettage specimens (51 GCTBs, 38 CBAs and 28 ABCs) were collected from the archives of the Calgary Laboratory Services/University of Calgary (31 cases, 2009-present) and Vanderbilt University Medical Center (86 cases, 1999-2010). Diagnostic cytology specimens were available for 9 patients (8 GCTBs and 1 CBA). PCR was conducted to amplify the region of interest in *H3F3A* or *H3F3B* followed by a SNaPshot© to interrogate each nucleotide in *H3F3A* codon 34 and *H3F3B* codon 36. All GCTBs and 18 ABCs were tested for *H3F3A* mutations; all CBAs and 10 ABCs were tested for *H3F3B* mutations.
Results: 36/51 GCTBs (71%) had an *H3F3A* G34W mutation. 33/38 CBAs (87%) had an *H3F3B* K36M mutation. Of 33 ABCs, one showed an *H3F3A* G34W mutation, which may represent a pre-existing GCTB. All 9 pre-curettage cytology specimens showed concordant molecular findings with the subsequent curettage (8 positive, 1 negative) and 3 repeat curettages also showed concordant molecular findings (2 positive, 1 negative). Of note, one of the cytology specimens was initially diagnosed as consistent with GCTB, but the diagnosis was changed to CBA upon curettage; both specimens were positive for *H3F3B* K36M. 3 curettage specimens with indeterminate features (2 favoring CBA, 1 favoring GCTB) were tested for both *H3F3A* and *H3F3B* mutations. Each was positive for only one mutation, helping to clarify the diagnosis.
Conclusions: These findings support the diagnostic utility of the *H3F3A* G34W mutation for GCTBs, and the *H3F3B* K36M mutation for CBAs. Testing for these mutations could prove a useful adjunct to histologic assessment in challenging cases. This is especially true in cytology specimens, where minimal material may preclude a definitive morphologic diagnosis but molecular testing is still possible.

81 Immunohistochemical Profile of Littoral Cell Angioma of the Spleen. A Report of 25 Cases Predominantly Associated with Visceral Malignancies

Kvetoslava Peckova, Michael Michal, Ladislav Hadravsky, Saul Suster, Ivan Damjanov, Michal Michal. Charles University, Medical Faculty and Charles University Hospital, Plzen, Czech Republic; Medical College of Wisconsin, Milwaukee, WI; The University of Kansas School of Medicine, Kansas City, KS.
Background: Littoral cell angioma (LCA) is a rare primary splenic vascular tumor frequently associated with internal malignancies. LCA demonstrates non-specific morphology. Immunohistochemistry (IHC) can prove distinct hybrid endothelial/histiocytic phenotype of littoral cells and helps to render the right diagnosis. We present a group of 25 LCA with a detailed immunohistochemical analysis and an emphasis on their frequent association with visceral malignancies.
Design: 25 original cases of LCA were collected from various institutions. All cases were examined by light microscopy and 17/25 cases with available tissue blocks were immunohistochemically stained for endothelial and histiocytic markers. Clinical data and follow-up were retrieved from respective institutions.
Results: Patients were 16 males, 9 females with age range 32-86 years (mean 56.2). Follow up was available for 23/25 patients, range 1-21 years (mean 8.6). All tumors had a multinodular cystic appearance with the size of the nodules ranging from 0.2 to 4 cm. Morphology fulfilled current histological criteria for LCA. All cases were positive for LYVE 1, FVIII, Fli-1, VEGFR 2 and 3, Claudin 5, ERG, LMO2, CD31, CD163, CD 11c, Lysozym, CD4 and negative for D2-40. 15/25 cases were associated with various malignancies including epithelial, mesenchymal and hematological.
Conclusions: The use of additional and hitherto unemployed endothelial and histiocytic markers enlarged the spectrum of IHC features of LCA, which may facilitate the diagnosis. Throughout clinical evaluation for a concomitant visceral malignancy is recommended in every patient diagnosed with LCA, as more than half of the cases in the current study revealed a co-existent visceral malignancy. The cohort of 25 patients with LCA is, to our knowledge, the largest series published to date.

82 P16 Expression as a Prognostic and Predictive Marker in Osteosarcoma of Bone

Alberto Righi, Marco Gambarotti, Marta Sbaraglia, Andrea Sisto, Stefano Ferrari, Piero Picci, Paolo Dei tos. Department of Pathology, Rizzoli Institute, Bologna, Italy; Department of Pathology, Treviso Regional Hospital, Treviso, Italy; Department of Oncology, Rizzoli Institute, Bologna, Italy; University of Eastern Piedmont, Polis-Public Policy and Choice, Alessandria, Italy.
Background: The potential prognostic and predictive value of p16 (p16INK4a) in high grade osteosarcoma of bone has been recently investigated in small series and the results from different studies were somewhat controversial.
Design: Immunohistochemical analysis of p16 expression was performed in a series of 357 cases of high grade osteosarcoma of bone (grade 3 according to World Health Organization, grade 4 according to Broders system) to explore its potential prognostic

and predictive value. The main criteria of selection was the availability of adequate material from both the initial biopsy and the post-chemotherapy surgical sample to allow morphologic and immunohistochemical characterization. Immunohistochemistry was performed with a commercially available p16 monoclonal mouse antibody. Follow-up data were available in all cases with a mean of 120 months (range: 6-366 months).
Results: Positivity for p16 was detected in 70.6% (252/357) of cases. A significant association was noted between p16 expression and pathologic complete response to chemotherapy (chi-square test 25.307; P< 0.001); conversely, no association could be established between p16 expression and age, gender, tumor site and histologic subtype. Kaplan-Meier survival analysis demonstrated that the absence of p16 expression was significantly associated with an adverse metastases free survival (p=0.012), disease free survival (p=0.04) and overall survival (p=0.05) when compared with the presence of p16 expression. Multivariate Cox regression analysis did not estimated p16 expression to be an independent prognostic and predictive factor (hazard ratio (HR)= 1.422 for metastases free-survival (MFS), p=0.052; HR= 1.288 for disease free-survival (DFS), p=0.181; HR= 1.322 for overall survival (OS), p=0.179) at difference to pathologic response to chemotherapy that represented the only independent prognostic factor in our series (HR= 1.933 for MFS, p<0.001; HR= 2.145 for DFS, p<0.001; HR= 2.395 for OS, p<0.001).
Conclusions: Our data indicate that: 1.immunohistochemical expression of p16 in high-grade osteosarcoma significantly correlates with histologic response to chemotherapy. 2. p16 immunonegativity is associated with worse prognosis although it does not represent an independent prognostic biomarker.

83 Exploring Intra-Tumor Heterogeneity in Neurofibromatosis Type 1 Plexiform Neurofibromas: Integration of Histological and Genomic Data Reveals Correlation between Progressive Loss of CDKN2A and Degree of Cellular Atypia

Cleofe Romagosa, Meritxell Carrio, Ernest Terribas, Bernat Gel, Cristina Flamerich, Teresa Moline, Inma Rosas, Elisabeth Castellanos, Conxi Lazaro, Eduard Serra. Hospital Universitari Vall d'Hebron, Barcelona, Spain; Institut de Medicina Predictiva i Personalitzada del Càncer (IMPPC), Barcelona, Spain; Hereditary Cancer Program, Institut Català d'Oncologia (ICO-IDIBELL), Barcelona, Spain.
Background: Plexiform neurofibromas (PNFs) are one of the major complications of patients with Neurofibromatosis type 1 (NF1). PNFs affect more than 40% of NF1 patients and a subgroup of them undergo malignant transformation. Contrary, dermal neurofibromas (DNF), never progress towards malignancy. Regarding genomics and transcriptomics, DNFs and PNFs are very much alike. So what is different among these tumors that confer PNFs a risk to become malignant? One possibility is that the large extension of affected tissue may be hiding intra-tumor molecular heterogeinity present in PNFs that would result in malignat transformation.
Design: With the aim of exploring the histological and molecular variation within PNFs we histologically characterized 8 plexiform neurofibromas, previously divided in multiple sections. Cellular density, atypia and other morphologic aspects were evaluated. S100, ki67, p16 and p53 were evaluated by immunohistochemistry in 2-3 sections of each PNF. In addition, a genomic characterization (SNP-array analysis and exome sequencing) was performed in each of the selected sections to allow an integration of histological and genomic data for evaluating intra-tumor variability.
Results: PNFs exhibited a different degree of intra-tumor histological and biological diversity. Genome integrity of the different PNFs was almost non-altered, with the exception of the *NF1* locus and long arm of chromosome 17, where the *NF1* gene is located. Cell density and atypia were correlated with molecular genetic findings, and 2/8 cases showed morphological and genetic intra-PNF heterogeneity. In PNF3, sections with higher cellular density and atypia were correlated with the presence of higher percentages of $NF1^{-/-}$ Schwann cells (SC), according to S-100 staining and BAF plots from SNP-arrays, and lower density areas with higher proportion of $NF1^{+/-}$ SC. In PNF4, the increasing degree of atypia exhibited in different sections was correlated with the progressive loss of the *CDKN2A* loci.
Conclusions: The present study shows for the first time the existence of molecular heterogeneity within a PNF. Moreover, we identified the progressive loss of *CDKN2A* as one of the first molecular events after the loss of *NF1* that correlates with the degree of cellular atypia at histological level.

84 RNA-Sequencing Identifies ETV6-NTRAK3 as a Gene Fusion Involved in Gastrointestinal Stromal Tumors

Sabrina Rossi, Monica Brenca, Maurizio Polano, Daniela Gasparotto, Dominga Racanelli, Lucia Zanatta, Laura Valori, Stefano Lamon, Roberta Maestro, Angelo P Dei Tos. Treviso General Hospital, Treviso, Italy; CRO National Cancer Institute, Aviano, Italy.
Background: The vast majority of gastrointestinal stromal tumors (GIST) are driven by oncogenic activation of *KIT*, *PDGFRA* or, very rarely, *BRAF*. Loss of succinate dehydrogenase complex activity has been identified in a subset of *KIT/PDGFRA/BRAF*-mutation negative GIST. Yet, there is a significant fraction of GIST devoid of such alterations. We sought to explore the possible involvement of fusion genes in this "quadriple-negative" subgroup.
Design: RNA-sequencing was performed on FFPE samples from 5 quadriple-negative GIST. FusionCatcher, ChimeraScan and a in-house algorithm were used to identify fusion transcripts. RT-PCR and FISH were used to confirm interesting positive hits. Ectopic expression of interesting chimeras in HT1080 and U2OS was used to address their biological significance.
Results: RNA-sequencing unveiled the presence of a *ETV6-NTRK3* gene fusion in one out of 5 cases analyzed. The fusion encompassed exon 4 of ETV6 and exon 14 of NTRK3, thus differing from classical infantile fibrosarcoma-associated ETV6-NTRK3 chimera (ETV6 exon 5-NTRK3 exon 15). *ETV6* rearrangement was confirmed by FISH, with the vast majority of tumor cells showing *ETV6* split signal. *ETV6-NTRK3* breakpoint was confirmed by Sanger sequencing of the RT-PCR products. The index case was located in the rectum, featured an epithelioid morphology, showed a strong and diffuse expression of CD117 and DOG1, and fell in the high risk category based on AFIP criteria. No additional *ETV6*-rearranged cases were identified by FISH in a independent series of 26 GIST, tentatively enriched for *KIT/PDGFRA/BRAF*-mutation negative (4) and rectal cases (4). Intriguingly, similar to what reported for the infantile fibrosarcoma chimera, also the ET*V6-NTK3* fusion in our index case triggered activation of IGF1R signaling pathway and sensitized HT1080 and U20S cells to IGFR and ALK/MET inhibitors (Crizotinib and Certinib).
Conclusions: To the best of our knowledge this is the first report of an oncogenic gene fusion, namely *ETV6-NTRK3*, involved in GIST. The index case was a rectal and quadriple-negative GIST. Cell modeling of the fusion highlighted a role for the chimera in the sensitization to IGFR and ALK/MET inhibitors. Overall, our data suggest that the *ETV6-NTRK3* fusion might identify a rare subset of GIST with peculiar clinicopathological characteristics (quadriple negative and rectal location) which could be eligible for unprecedented targeted approaches.

85 Histology and Fusion Status in Metastatic Rhabdomyosarcoma

Erin R Rudzinski, James Anderson, Doug Hawkins. Seattle Children's Hospital, Seattle, WA; Frontier Science and Technology Research Foundation, Madison, WI; University of Washington and Fred Hutchinson Cancer Research Center, Seattle, WA.
Background: Recent studies on intermediate risk rhabdomyosarcoma (RMS) highlight the shift in the diagnostic criteria of alveolar RMS (ARMS) which occurred between 1997 and 2007 following publication of the International Classification of Rhabdomyosarcoma. This shift resulted in over-diagnosis of ARMS enrolled on Children's Oncology Group (COG) RMS trials during this period. These studies also confirmed that intermediate risk patients with fusion negative ARMS have an outcome similar to embryonal RMS (ERMS) and a superior event free survival to ARMS with either a PAX3 (P3F) or PAX7 (P7F) - FOXO1 fusion. The goal of the current study was to assess the impact of this diagnostic shift and the effect on outcome for patients with metastatic disease enrolled on two completed high-risk clinical protocols conducted between the years 1999 and 2010.
Design: We conducted a histologic re-review for patients with known fusion status including 82 patients enrolled on the high risk COG RMS study D9802 (1999-2004) and 62 patients enrolled on the subsequent high risk COG study ARST0431 (2006-2010). An additional 34 patients enrolled on ARST0431 did not have pathologic material for re-review but did have an original central pathology review diagnosis and were used in the outcome analysis.
Results: Approximately 20% of patients (18/82) enrolled on D9802 with an original diagnosis of ARMS were reclassified as ERMS. In contrast, 5% of patients (3/62) enrolled on ARST0431 with an original diagnosis of ARMS were reclassified as ERMS. 5 year event-free survival (EFS) for all patients with high-risk RMS was approximately 25%. However, for patients with confirmed or re-classified ERMS the EFS was 45% v. 30% for fusion negative ARMS, 20% for patients with P7F and 10% for patients with P3F (p=0.020). When analyzed by fusion status alone, EFS was approximately 40% for patients with fusion negative RMS v. 10% for patients with fusion positive RMS (p=0.001). Patients with ERMS treated on D9802 had an inferior outcome to those treated on ARST0431 (25% v. 60% EFS, p=0.012).
Conclusions: The discordance in diagnostic re-classification for COG study D9802 v. ARST0431 highlights the overdiagnosis of ARMS for patients enrolled on COG clinical trials between 1997 and 2007. Studies performed after this have reliable central pathology review data. As seen for intermediate risk RMS, patients with high risk fusion negative RMS have a superior outcome than RMS patients with either a P3F or P7F fusion.

86 CIC-DUX4 Fusion-Positive Round Cell Sarcomas of Soft Tissue and Bone: Clinicopthologic and Molecular Analysis from a Single Institution

Marta Sbaraglia, Marco Gambarotti, Stefania Benini, Gabriella Gamberi, Stefania Cocchi, Emanuela Palmerini, Davide Donati, Piero Picci, Daniel Vanel, Stefano Ferrari, Alberto Righi, Angelo P Dei Tos. Treviso Regional Hospital, Treviso, Italy; Rizzoli Institute, Bologna, Italy.
Background: Round cell sarcomas lacking specific translocations of Ewing sarcoma (EWS) are classified in the current WHO classification as "undifferentiated round cell sarcomas (URCS)" and represent a diagnostic challenge. Recently *CIC* gene (most often but not exclusively with *DUX4*) rearrangement has been identify in a subset of URCS. To date fifty-nine cases of *CIC-DUX4* positive sarcomas (CDS) have been reported, all arose in soft tissue or rarely in visceral sites.
Design: Fifty-one cases of URCS of bone and soft tissue treated in our institution from 1982 and 2014, lacking *EWSR1* or *FUS* gene rearrangement with available frozen tissue were retrieved. All cases were analyzed immunohistochemically for CD99 and WT1 and molecularly for the presence of the *CIC-DUX4* translocation by quantitative real time RT-PCR (qRT-PCR) analysis.
Results: Nineteen cases were not adequate for molecular analysis due to absence of neoplastic cells in the frozen sample; 25 were negative and 7 showed the presence of the *CIC-DUX4* chimeric transcript. The presence of *CIC* gene rearrangement was confirmed by FISH analysis in all cases. Patients' age ranged from 15 to 44 years (median: 33). Male to female ratio was 3:4. All but one case arose primarily in the soft tissue. Importantly one case originated from the right acetabulum, thus representing the first primary bone CDS reported to date. Morphologically, all cases showed an undifferentiated round cell population, arranged in nodules separated by fibrous septa, with abundant geographic necrosis, and multifocal nuclear pleomorphism. Occasional myxoid change of the stroma was seen. The tumors were focally positive or negative for CD99, and all but two showed cytoplasmic and/or nuclear immunoreactivity for WT1

(n-terminus). Five patients had lung metastases at presentation. All patients received chemotherapy in accordance to Ewing sarcoma protocols. All but one patient died of disease after a mean of 13 months from diagnosis (range: 6-20 months).
Conclusions: We describe seven new cases of CDS among which the first example of bone primary. Our series confirms that CDS is a very aggressive tumor with clinical, histological, and genetic distinctive features that justify separation from EWS.

87 The Diagnostic Utility of CAMTA1 and TFE3 Immunohistochemistry in Epithelioid Vascular Tumors

Marta Sbaraglia, Marco Gambarotti, Alberto Righi, Angelo P Dei Tos. Treviso Regional Hospital, Treviso, Italy; Rizzoli Institute, Bologna, Italy.
Background: Epithelioid vascular tumors represent a broad spectrum of mesenchymal lesions that includes benign (epithelioid hemangioma EH), low grade malignant (epithelioid hemangioendothelioma EHE) and high grade malignant (epithelioid angiosarcoma AS). Correct diagnosis is often challenging, however the presence of specific molecular aberrations involving the *CAMTA1* and *TFE3* genes has been reported in EHE. Immunohistochemistry for CAMTA1 and TFE3 may surrogate molecular analysis and represent a key finding in sorting out difficult cases.
Design: Sixty cases of epithelioid vascular tumor were retrieved. Whole sections from formalin-fixed, paraffin embedded material were immunostained for CD31, ERG, CAMTA1 and TFE3. Moderate to strong nuclear staining for CAMTA1 and TFE3 was scored as positive.
Results: Following diagnostic reappraisal 15 EHE (3 involving long bones and 12 affecting visceral and soft tissue sites), 30 EAS (3 involving bones and 27 visceral and soft tissue sites) and 13 EH cases (1 involving bone and 12 the skin of the head and neck region) were identified. Two cases were reappraised as pseudomyogenic hemangioendothelioma and therefore excluded. One out of 3 EHE of bone and 9/12 EHE of soft tissue were CAMTA1 positive. None of other epithelioid vascular tumors (53/53) showed CAMTA1 immunopositivity. Strong nuclear TFE3 expression was observed in one CAMTA1- negative EHE of bone as well as in one CAMTA1- negative EHE of soft tissue. TFE3 was negative in all other cases.
Conclusions: When dealing with epithelioid vascular tumors, nuclear expression of CAMTA1 and TFE3 seems to be highly specific for EHE. CAMTA1 And TFE3 appears to be mutually exclusive, and both represent helpful markers in the histopathologic classification of epithelioid vascular tumors.

88 Identifying Unique Genome Abnormalities That Distinguish Enchondroma from Chondrosarcoma

John Scarborough, Robert Ricciotti, Yu Wu, Yuhua Liu, Benjamin Hoch, Yajuan Liu, Eleanor Chen. University of Washington, Seattle, WA.
Background: Distinguishing enchondroma from grade 1 and even grade 2 conventional chondrosarcoma based on histologic features can be a diagnostic challenge, but has strong implications for clinical management. Enchondroma, a benign cartilage neoplasm, is usually cured by simple curettage. In contrast, chondrosarcoma is a malignant neoplasm of bone which tends to locally recur and may metastasize. There remains a need for an ancillary molecular tool to help distinguish enchondroma from chondrosarcoma.
Design: SNP-based cytogenomic microarray analysis (CMA) using the Illumina Infinium CytoSNP-850K platform was performed on genomic DNA isolated from formalin-fixed paraffin-embedded tissue of 5 cases of enchondroma and 8 cases of chondrosarcoma. Chondrosarcomas were characterized by bone invasion/entrapment on microscopic examination and aggressive features on imaging. Enchondromas lacked invasive growth and were confined to bone. For each case, a log intensity ratio and allele frequency were generated to represent net copy number changes and regional genetic abnormalities (e.g. aneuploidy, deletion, amplification and loss-of-heterozygosity). To represent genomic complexity of each case, a genomic index (GI) of (total number of alterations)^2/total number of involved chromosome was determined.
Results: All enchondroma cases (5 short bones and 1 long bone; age range: 18-57; sex: 3 F/ 2 M) showed no copy number changes or
regional genetic abnormalities. By contrast, all chondrosarcoma cases (1 grade 1, 6 grade 2 and 1 grade 3; 1 long bone, 1 vertebral column, 2 short bones, 4 flat bones; age range: 20-77; sex: 5 F/ 3 M) demonstrated complex genetic alterations with frequent chromosomal losses. Recurrent chromosomal alterations in at least 50% of cases include losses of 6q and 13 (100%), loss of 1p, 6p, 9p and 11 (83%), loss of 1q, 3, 4p, 9q, 10, and 22 (67%) and loss of 4q, 14, 16q, 17, and 21 (50%). One metastatic chondrosarcoma was characterized by 3 whole-chromosome losses and 10 partial deletions. Chondrosarcoma cases demonstrated GI ranging from 4 to 20.06 and appeared not to correlate with grade.
Conclusions: SNP-based CMA demonstrates complex copy number and regional genetic alterations, including recurrent loss of 6q and 13, in chondrosarcoma in contrast to no abnormalities in enchondroma. Stratification of genetic complexity by the GI clearly distinguishes enchondroma from chondrosarcoma, but does not differentiate low-grade from high-grade chondrosarcoma. SNP CMA is a potentially useful molecular test to distinguish enchondroma from chondrosarcoma in diagnostically challenging cases.

89 Loss of H3K27 Trimethylation Distinguishes Malignant Peripheral Nerve Sheath Tumors from Histologic Mimics

Inga-Marie Schaefer, Christopher Fletcher, Jason L Hornick. Brigham and Women's Hospital/Harvard Medical School, Boston, MA.
Background: The differential diagnosis of malignant peripheral nerve sheath tumor (MPNST) is challenging, particularly in the sporadic setting and in the absence of supportive markers. Inactivation of the polycomb repressive complex (PRC) 2, resulting from inactivating mutations of its constituents *SUZ12* or *EED1,* has recently been identified in 70-90% of MPNST. Homozygous PRC2 inactivation results in loss of histone H3K27 trimethylation (H3K27me3). PRC2 inactivation promotes tumor progression and may render patients sensitive to epigenetic-based targeted therapies. H3K27me3 loss has not yet been validated as a diagnostic marker of MPNST.
Design: We performed immunohistochemistry using a rabbit monoclonal antibody directed against trimethylated lysine 27 of histone H3 (1:500 dilution; clone 07-449; Millipore) in 100 MPNST (70 sporadic, 10 neurofibromatosis type 1 (NF1)-associated, 10 radiation-associated, 10 epithelioid; 31 low, 36 intermediate, 33 high grade) and 200 other benign and malignant spindle cell neoplasms that represent potential mimics (20 each monophasic synovial sarcoma, leiomyosarcoma, dedifferentiated liposarcoma, malignant solitary fibrous tumor, low-grade fibromyxoid sarcoma, cellular schwannoma, spindle cell melanoma, unclassified post-radiation sarcoma; 10 each atypical neurofibroma, spindle cell rhabdomyosarcoma, gastrointestinal stromal tumor, fibrosarcomatous dermatofibrosarcoma protuberans).
Results: In total, 51 (51%) MPNST, including 34 (49%) sporadic, 7 (70%) NF1-associated, 10 (100%) radiation-associated, and no epithelioid MPNST were negative for H3K27me3. An additional 6 (6%) MPNST showed heterogeneous H3K27me3 expression. Among the 90 sporadic, NF1-associated, and radiation-associated MPNST, complete H3K27me3 loss was observed in 29% of low grade, 59% of intermediate grade, and 83% of high grade tumors (low vs. intermediate/high grade, $P = 0.0003$). Among other tumor types, 4 (20%) unclassified post-radiation sarcomas were negative for H3K27me3, whereas all other neoplasms were positive.
Conclusions: Loss of H3K27me3 is highly specific for MPNST (although only modestly more sensitive than S-100 protein and SOX10) and may be a useful diagnostic immunohistochemical marker. Our findings suggest that PRC2 inactivation in MPNST may occur during progression to higher grades. Detection of H3K27me3 loss in previously unclassified radiation-associated sarcomas indicates that a subset of these tumors may represent MPNST. The value of H3K27me3 as a predictive marker for sensitivity to epigenetic-based therapies remains to be determined.

90 Non-syndromic Low-Flow Mixed Venous/Lymphatic Malformation of Skeletal Muscle of the Extremity (Fibro-Adipose Vascular Anomaly): A Clinicopathologic Study of 11 Cases with Emphasis on Distinctive Morphologic Features

Michael L Schwalbe, Lara N Mrak, Paula E North, Darya Buehler. University of Wisconsin School of Medicine, Madison, WI; Children's Hospital of Wisconsin, Milwaukee, WI.
Background: Non-syndromic low-flow vascular malformations of skeletal muscle are often misdiagnosed as cavernous hemangiomas or arteriovenous malformations (AVMs), which may impact management. Recently, a subtype of intramuscular mixed venous/lymphatic malformation was described and termed "fibro-adipose vascular anomaly" (FAVA). Here we report 11 new cases consistent with this lesion and emphasize its distinct morphologic features and prominent lymphatic component.
Design: Cases diagnosed as cavernous hemangioma or malformation of skeletal muscle of the limb were retrieved and histologic features re-evaluated in conjunction with a vascular anomaly expert. Clinical, imaging, operative and follow-up data were obtained. Cases with high-flow imaging characteristics or history of PTEN/other syndromes were excluded. D2-40 immunostain and elastic stain were performed. Nine ordinary intramuscular venous malformations (VMs) were studied for comparison.
Results: Eleven patients (9F, 2M), median age 21 years (range 0-50), presented with significant pain (9/11, duration 6 mo-6 years). None had contractures. Locations included deep muscle of the calf (5), distal thigh (3), forearm (2) and foot (1). All cases showed a VM with clusters of thin "honeycomb" veins and fibrofatty change (11/11), conspicuous abnormal lymphatics confirmed by D2-40 immunostain (9/10), lymphoid aggregates (10/11), and hemosiderin deposits (9/11). Eight cases showed distinctive indeterminate vessels with concentric hypertrophy and narrow lumina resembling small arteries but with absent/aberrant internal elastica. Two cases had ossification. Venous thrombi were rare (2/11). In contrast, ordinary VMs showed large collapsed veins with frequent thrombi (9/9) and rare "honeycomb" veins (2/9), lymphoid aggregates (1/9) and focal lymphatics (2/9). Fibrosis was present in 2/9 and hemosiderin in 4/9 ordinary VM. Indeterminate vessels were suggested only focally in one case. Six of 9 ordinary VMs were painful, indicating that the latter is not a reliable criterion to separate these lesions.
Conclusions: Non-syndromic intramuscular mixed venous/lymphatic malformations, for which the designation "FAVA" has been suggested, has distinctive clinico- and histopathologic features which set it apart from ordinary intramuscular VMs. The distinctive indeterminate vessels resemble arteries; however, these are low-flow lesions and should not be misinterpreted as AVMs.

91 SIRT5 Is Required for Viability of the Ewing Sarcoma Cell Line A673 and the Osteosarcoma Cell Line U2OS

David Seward, Sarah Bergholtz, Elizabeth Pederson, Mary Skinner, Jeongsoon Park, Elizabeth R Lawlor, David Lombard. University of Michigan, Ann Arbor, MI.
Background: Sirtuins are a diverse family of enzymes possessing a range of biological functions, biochemical activities, and protein targets. While best known as deacetylases with roles in lifespan extension, the extent of their impact on metabolic pathways has increasingly been appreciated. It is now established that acetyl groups are only one of many post-translational modifications targeted by sirtuins. For example, it has recently been demonstrated that SIRT5 is unique among the mammalian sirtuins in that it preferentially removes succinyl, malonyl, and glutaryl groups from modified lysine residues. A collaborative mass spectrometry study from our lab comparing the succinylome in SIRT5-deficient and -proficient cells identified potential SIRT5 targets *in vivo*. One intriguing candidate pinpointed by this screen was the E1α subunit of the pyruvate dehydrogenase complex (PDC). We subsequently showed that SIRT5 functions to modulate PDC activity *in vitro* and *in vivo* via E1α desuccinylation.

Functional suppression of PDC activity is a relatively common event in cancer and is an established mechanism that contributes to metabolic reprogramming. In our current work, we investigated whether SIRT5 is required for viability in two sarcoma cell lines.
Design: We used a lentiviral vector system to deliver shRNAs targeting SIRT5 in the U2OS and A673 cell lines. Cell viability was quantified over time with the WST-1 spectrophotometric assay. All experiments were accompanied by parallel controls, including cells infected by non-targeting shRNAs and uninfected control groups. Statistical analyses were completed using the t-test.
Results: shRNA mediated knock-down of SIRT5 results in a dramatic, rapid decrease in cell viability relative to controls in both the U2OS and A673 cell lines ($p<0.0001$).
Conclusions: Our preliminary data support the hypothesis that SIRT5 is required for viability in U2OS and A673 sarcoma cell lines. We hypothesize the mechanism involves metabolic reprogramming mediated by SIRT5 desuccinylation. Specifically, we believe SIRT5-mediated desuccinylation of the E1α subunit represents an important regulatory switch that inactivates the PDC and suppresses mitochondrial respiration, thereby providing crucial precursors for macromolecular synthesis, without which the cells die. As a result, SIRT5 may represent a therapeutic target for the treatment of sarcomas. Efforts to identify compounds that inhibit SIRT5 enzymatic activity are ongoing.

92 Leiomyosarcomas and Rhabdomyosarcomas Over-Express Nicotinamide Phosphoribosyltransferase

Rodney E Shackelford, Rabie Shanti, Junaid Ansari, Moiz Vora. LSU Health Sciences, Shreveport, LA; Feist Weiller Cancer Center, Shreveport, LA.
Background: Nicotinamide Phosphoribosyltransferase (Nampt) is over-expressed in a variety of malignancies, including ovarian, gastric, thyroid, colorectal, esophageal, breast cancers, and several lymphomas. Nampt catalyses the rate-limiting step of nicotinamide adenine dinucleotide synthesis (NAD) promoting cell growth and division. To our knowledge, no one has examined Nampt levels in any sarcoma type. Here we examined Nampt expression by immunohistochemistry (IHC) in normal skeletal and smooth muscle, benign leiomyomas, leiomyosarcomas, and rhabdomyosarcomas.
Design: Tissue microarrays (TMAs) were purchased form US Biomax, which collectively had approximately 60 benign smooth and skeletal muscle, and leiomyoma, leiomyosarcoma, and rhabdomyosarcoma samples from different patients. The TMAs were subject to IHC analysis. The mouse primary monoclonal anti-Nampt antibody (#ALX-804-717, Plymouth Meeting, PA) was used, with a secondary anti-mouse antibody. Relative Nampt protein IHC expression was determined as the product of immunostain intensity and percent of cells stained. Both were scored on a 0-3 scale, with 3 being maximal. Immunostain intensity was scored with no staining being 0, light staining as 1, moderate staining as 2, and heavy staining as 3. The percent of cells stained was measured with no detectable staining as 0, 1-33% as 1, 34-66% as 2, and 67-100% as 3.
Results: Nampt levels were very low in benign smooth and skeletal muscle, slightly elevated in benign leiomyomas, and significantly elevated in leiomyosarcomas and rhabdomyosarcomas. Interestingly, Nampt levels were higher in high-grade leiomyosarcomas compared to low-grade. Additionally differences in Nampt staining were found between different rhabdomyosarcoma subtypes.
Conclusions: Nampt protein levels are elevated in several different malignancies, with some data indicating that higher Nampt levels correlate with a worse prognosis, chemotherapy resistance, and a greater likelihood for metastasis and local invasion. Here we show that Nampt levels are increased in leiomyosarcomas and rhabdomyosarcomas, with the grade of leiomyosarcoma and rhabdomyosarcoma subtype correlating with specific Nampt
expression levels. Nampt activity is necessary for NAD production and hence tumor growth. Since Nampt inhibitors have been used to treat human malignancies, our data indicates that such therapy might have value in treating leiomyosarcomas and rhabdomyosarcomes.

93 Single Institutional Analysis of Prognostic Factors for Soft Tissue Sarcoma; Debatable Value of Tumor Depth

Yoshiya Sugiura, Noriko Motoi, Keisuke Ae, Hiroaki Kanda, Seiichi Matsumoto, Rikuo Machinami, Yuichi Ishikawa. The Cancer Institute, Tokyo, Japan; The Cancer Institute, Hospital, Tokyo, Japan.
Background: Histologic grade, tumor size, tumor depth, nodal involvement, remote metastasis are prognostic factors of soft tissue sarcoma. These factors are included in AJCC staging system for soft tissue sarcoma. However recently prognostic value of tumor depth has been questioned. In this study we re-evaluate the value of these factors.
Design: Sixty hundred and five patients with soft tissue sarcoma were included. We performed survival analysis using prognostic factors: histologic grade according to FNCLCC grading system, age, sex, site, depth, size, venous invasion, nodal involvement, and remote metastasis. We used Kaplan-Meiyer' s method, Log-Rank test, and Cox's proportional hazard model. Time of origin was the day of operation with curative intent and endpoint was the day of tumor mortality. Death from other causes was considered as censoring.
Results: In univariate analysis, Histologic grade($p<0.001$), size($p<0.001$), depth($p=0.011$), venous invasion($p<0.001$), nodal involvement($p<0.001$), and remote metastasis($p<0.001$) were significant prognostic factors. In multivariate analysis, histologic grade (Grade2: Relative risk (RR) = 8.514 $p<0.001$; Grade3: RR=17.515 $p<0.001$), size (RR=1.892 $p=0.009$) were independent predictors, but depth (RR=1.340 $p=0.217$) was not. In chi-square test, size and depth were significantly related ($p<0.001$). Furthermore, when patients were dichotomized according to size(≤5cm vs. >5cm), depth was no longer a significant factor in univariate analysis. These results suggest that tumor depth is only a confound factor related to tumor size.

Prognostic factors		Relative risk (RR)	p-value
Histologic grade	Grade2/grade1	8.514	<0.001
	Grade3/grade1	17.515	<0.001
	Grade3/grade2	2.102	<0.001
Site	extremity/trunk	0.983	0.94
Depth	superficial/deep	1.34	0.217
Size	≤5cm/>5cm	1.892	0.009
Venous invasion	+/-	2.555	<0.001
Nodal involvement	+/-	3.024	<0.001
Remote metastasis	+/-	2.193	<0.001

Conclusions: 1. Tumor depth is included in AJCC/UICC staging system. But its value should be re-evaluated. 2. Venous invasion may be a useful prognostic factor. Its value should also be evaluated more precisely.

94 Expression of Enhancer of Zeste Homolog 2 (EZH2) Protein and Intracellular Signaling Molecules p-ERK, MYC, and p-STAT3 in Histiocytic and Dendritic Cell Neoplasms

Xuejun Tian, Jason L Hornick, Christopher Fletcher, Jie Xu, Ali Shahsafaei, David M Dorfman. Brigham and Women's Hospital, Harvard Medical School, Boston, MA; MD Anderson Cancer Center, Houston, TX.
Background: EZH2, a member of the polycomb protein group, is an important methyltransferase that is over-expressed in various carcinomas and hematopoietic neoplasms. Here we investigated EZH2 expression in the range of histiocytic and dendritic cell neoplasms and correlated its expression with that of p-ERK, MYC, and p-STAT3, potential regulators of EZH2 expression.
Design: Immunohistochemical staining (IHC) for EZH2 was performed on 63 cases of histiocytic and dendritic cell neoplasms, including blastic plasmacytoid dendritic cell neoplasm (BPDCN, 12), histiocytic sarcoma (HS, 17), follicular dendritic cell sarcoma(FDCS, 15), langerhans cell histiocytosis(LCH, 16), interdigitating dendritic cell sarcoma(IDCS, 3), and 9 cases of benign histiocytic diseases, using formalin fixed, paraffin-embedded tissue. We subsequently performed IHC for p-ERK, p-STAT3, and MYC on these neoplasms.
Results: In histiocytic and dendritic cell neoplasms, 41-67% of cases showed strong EZH2 expression. With the exception of BPDCN, 60% to 80% of neoplastic cases showed strong p-ERK expression. Only a small percentage of cases (less than 30%) showed positivity for MYC or p-STAT3 in neoplastic cells. We next focused on cases with strong EZH2 staining, to determine if there was p-ERK, MYC, and/or p-STAT3 co-expression. In FDCS, LCH, and HS cases, 90%, 89%, and 70% of cases showed co-expression, respectively, of p-ERK with EZH2, while only a small percentage of these cases showed MYC or p-STAT3 co-expression with EZH2 (less than 30%). Interestingly, 9 cases of SHML and JXG did not show EZH2 expression.
Conclusions: EZH2 is strongly expressed in more than 50% of cases of histiocytic and dendritic cell neoplasms, but not in benign histiocytic conditions, suggesting that this molecule may function as an oncogenic protein in these neoplasms. However, unlike our previous study showing that EZH2 expression correlates with grade in B cell neoplasms, only 41% of cases of BPDCN, a clinically aggressive tumor, had high EZH2 expression, suggesting alternative mechanism(s) may contribute to tumorigenesis. Our study suggests that the p-ERK signaling cascade, but not those of MYC or p-STAT3, plays an important role in histiocytic and dendritic cell neoplasia, possibly through regulation of EZH2 expression. P-ERK and EZH2 signaling cascades may serve as therapeutic targets for the treatment of histiocytic and dendritic cell neoplasm.

95 Finding Fusions: A Promising Commercially Available NGS Sarcoma Panel

Ashley Windham, Kimberly L Walker, Linden L Watson, Arundhati Rao, Riyam T Zreik. Baylor Scott & White Hospital, Temple, TX.
Background: Diagnosis of bone and soft tissue (BST) tumors often requires multimodal ancillary studies including identification of associated chromosomal translocations using fluorescence in situ hybridization (FISH), cytogenetics and other molecular techniques. A commercially available next generation sequencing (NGS) sarcoma panel that targets 26 genes and identifies corresponding fusions was evaluated for its utility as an adjunct diagnostic tool in BST cases.
Design: Available slides from 50 BST cases, including biopsy and resection material, were identified and reviewed. Twenty-six cases were selected for sequencing with 20 of these cases having known translocations: myxoid/round cell liposarcoma (MLPS, n=3), synovial sarcoma (SS, n=6), alveolar rhabdomyosarcoma (ARMS, n=2), nodular fasciitis (NF, n=4), Ewing sarcoma (ES, n=2), and solitary fibrous tumor (SFT, n=3). The remaining six cases included five histologic subtypes with no known associated translocations. Formalin-fixed, paraffin embedded blocks were selected, the tumors were enriched by microdissection, and tumor RNA was extracted and subjected to the Archer™ FusionPlex™ Sarcoma Panel. The results were analyzed using the Archer™ Analysis software and compared to available fusion status results.
Results: The expected fusions were detected in 65% (13/20) of cases including SS (5/6), ES (2/2), SFT (2/3), NF (2/4), ARMS (1/2), and MLPS (1/3). A fusion was not detected in six cases. Five of those six cases were limited by either low coverage or poor quality RNA (ARMS n=1, NF n=1, MLPS n=2, SS n=1). One case had good quality RNA and good coverage (SFT n=1) but no fusion was detected. A novel fusion involving *USP6* was identified in one case of NF. A fusion was detected in only one of the six negative control cases in which a novel fusion involving *HMGA2* was found in well-differentiated liposarcoma. NGS identified an expected fusion in one case of SS in which FISH failed.

Conclusions: The NGS panel is a promising tool in identifying fusions in BST cases as we detected the expected results in 69% of the informative tested cases. Further optimization, particularly with regards to fixation and RNA extraction may improve the sensitivity of this assay. Although not without its limits, this panel is a potentially powerful tool in difficult to diagnose cases or cases with limited tumor cells.

96 Mass Spectrometry Highlights Proteomic and Epigenetic Changes upon PRC2 Loss in MPNST

John Wojcik, Simone Sidoli, Benjamin A Garcia, Kumarasen Cooper. Hospital of the University of Pennsylvania, Philadelphia, PA; University of Pennsylvania, Philadelphia, PA.

Background: The polycomb repressive complex 2 (PRC2) is a key epigenetic regulator and its dysfunction has been implicated in human malignancies. Recent work has established a central role for loss-of-function mutations in PRC2 components in the pathogenesis of MPNST. We have developed techniques to apply proteomics approaches to the study of FFPE tissue samples. We present a quantitative proteomic approach to the investigation of protein expression and histone post-translational modifications (PTMs) in a set of MPNST from our pathology archives.

Design: Neurofibromas and MPNST in patients with documented NF1 were selected following histologic review. Whole tissue sections of H&E as well as IHC stains for H3K27me3, desmin and myogenin were reviewed. Total cellular protein was isolated from FFPE tissue cores, digested and analyzed using nano-liquid chromatography and tandem mass spectrometry (LC-MS/MS). Histones were isolated by gel electrophoresis, in-gel digested and derivatized prior LC-MS/MS. Histone and PTM quantification were performed using lab-developed software. Statistical analysis was performed using Student's t-test and hypergeometric distribution of gene ontology annotations (DAVID and GOrilla software tools).

Results: 4/8 MPNSTs showed complete loss of H3K27me3 by immunohistochemistry and mass spectrometry. This included a complete loss of H3K27me3 in all four MPNST classified at triton tumors. Direct comparison of histone PTMs in an NF and an MPNST from the same patient revealed significant decreases in the histone marks H3K27me2, H3K9me3 and H3K9me2 in MPNST, all associated with gene repression. Comparative proteomic analysis of MPNSTs with and without H3K27me3 loss using hypergeometric distribution of gene ontology annotations showed increased expression of proteins involved in nucleosome and chromatin remodeling in tumors with loss of PRC2 activity.

Conclusions: Mass spectrometry reliably detects and quantifies global changes in histone modifications correlated with PRC2 loss of function in archived tumors. The loss of H3K27me3 was associated with an increase in proteins involved in chromatin and nucleosome reorganization, suggesting that PRC2 loss leads to altered genome organization in a subset of MPNSTs. Interestingly, triton tumors all showed H3K27me3 loss, suggesting that PRC2 loss facilitates divergent skeletal muscle differentiation.

97 ETV6 Gene Rearrangement in Inflammatory Myofibroblastic Tumor

Hidetaka Yamamoto, Akihiko Yoshida, Kenichi Kohashi, Yoshinao Oda. Kyushu University, Fukuoka, Japan; National Cancer Center Hospital, Tokyo, Japan.

Background: The aim of this study was to elucidate the pathological features of inflammatory myofibroblastic tumor (IMT) with the gene rearrangement other than *ALK*.

Design: We investigated ALK, ROS1, ETV6, NTRK3 and RET in 36 cases of IMT using immunohistochemical staining (IHC), fluorescence *in situ* hybridization (FISH) and reverse transcription-polymerase chain reaction (RT-PCR).

Results: ALK IHC and ROS1 IHC were positive in 22/36 (61.1%) and 2/36 (5.6%) cases, respectively. One case with ROS1 positivity showed cytoplasmic and dot-like ROS1 expression by IHC and the *TFG-ROS1* fusion transcript by RT-PCR. Two cases of pulmonary IMT, in a 7-year-old and a 23-year-old patient, had *ETV6* gene rearrangement, and the *ETV6-NTRK3* fusion transcript was confirmed in one case. These tumors were composed of biphasic myxoid and highly cellular areas with rich plasmacytic infiltration; the histological features were different from those of infantile fibrosarcoma. *RET* gene rearrangement was not detected.

Conclusions: These results suggest that a subset of ALK-negative IMTs have the gene rearrangement of *ROS1, ETV6* or *NTRK3* as a possible oncogenic mechanism, and that the detection of these alterations may be of diagnostic value and helpful for determining promising therapeutic strategies.

98 Establishment and Gene Expression Analysis of a Mouse Model for CIC-DUX4 Sarcoma

Toyoki Yoshimoto, Miwa Tanaka, Takuro Nakamura. The Cancer Institute, Japanese Foundation for Cancer Research, Tokyo, Japan; Toranomon Hospital, Tokyo, Japan.

Background: *CIC-DUX4* fusion-positive round cell tumor is a highly aggressive soft tissue tumor, historically labelled as Ewing-like sarcoma. To elucidate its biological features, and to differentiate it from Ewing sarcoma, we designed to establish an *ex vivo* mouse model expressing *CIC-DUX4*. By means of this model, we investigated comprehensive gene expression patterns to compare with Ewing sarcoma (ES) and normal tissue, and responsiveness to inhibitory drugs.

Design: The HA-tagged *CIC-DUX4* fusion cDNA was introduced into murine embryonic mesenchymal cells purified from soft parts using a retrovirus vector. The BALB/c mouse was subcutaneously transplanted with the infected cells. Gene expression profiles of CIC-DUX4 sarcoma (CDS) were analyzed by cDNA microarray and compared to those of the Ewing sarcoma model. Inhibitory drugs were screened using SCADS inhibitor kits.

Results: All the transplanted mice developed a solid tumor mass within 4 weeks. The tumor consisted of aggressive proliferation of HA-positive short spindle cells. Comparisons of gene expression profiles between CDS and ES, or between CDS and normal tissues indicated significantly up-regulated genes including *Etv1, Etv5, Vgf, Crh* and *Zic1*, known targets of CIC-DUX4. GSEA showed enrichment of gene sets for characteristic pathways such as cell cycle, adhesion and VEGF signaling in CDS. Immunohistochemistry revealed the distinctive expression of some molecules in CDS comparing with ES, identifying potential biomarkers for diagnosis of CDS. Several specific drugs showing efficient inhibitory effects for CDS cells were identified.

Conclusions: We successfully established mouse sarcoma model bearing CIC-DUX4 fusion and these results underscore usefulness of the mouse model and distinct biological features of CDS.

99 Expression of TLE-1 and CD99 in Carcinoma: Pitfalls in Diagnosis of Synovial Sarcoma

Daniel Zaccarini, Xiaobing Deng, Jamie Tull, Charlene Maciak, Alfredo Valente, Shengle Zhang. SUNY Upstate Medical University, Syracuse, NY.

Background: The characteristic immunoprofile for the diagnosis of synovial sarcoma, a neoplasm of unclear tissue origin, is expression of transducer-like enhancer of split 1 (TLE-1), CD99, partial expression of cytokeratin (CK), and epithelial membrane antigen (EMA) by immunohistochemistry (IHC). Diagnostic dilemma or misdiagnosis can occur due to overlap in IHC and morphology with carcinomas, and particularly poorly differentiated and metastatic tumors. The frequency of TLE-1 and CD99 expression in carcinomas by IHC has not been previously assessed. We evaluated TLE-1 and CD99 expression in various carcinomas and identified the expression of the SS18 (SYT) gene rearrangement (a characteristic biomarker for synovial sarcoma) in tumors positive for TLE-1 and/or CD99 expression.

Design: Immunostains of TLE-1 (Clone 1F5) and CD99 (Clone EPR3097Y) were performed in 100 various carcinomas including: 41 adenocarcinomas (ADCA), 14 squamous cell carcinomas (SqCC), 7 breast carcinomas, 5 thyroid carcinomas, 5 renal cell carcinomas (RCC), 5 hepatocellular carcinomas (HCC), 4 mucoepidermoid carcinomas (MEC), 4 urothelial cell carcinomas (UCC), 3 adrenocortical carcinomas (ACC), 2 basal cell carcinomas (BCC), 2 neuroendocrine carcinomas (NEC), 2 small cell carcinomas (SCC), 1 each for seminoma, adenosquamous carcinoma, intraductal papillary mucinous neoplasm, adenoid cystic carcinoma, ovarian serous carcinoma, and malignant mixed germ cell tumor. TLE-1 expression in ≥10% nuclei with ≥ moderate intensity was defined as positive, ≥10% nuclei with weak staining as equivocal, and < 10% as negative. Membranous CD99 expression was evaluated with the same cut-off values. SS18 gene rearrangements with break-apart FISH probe were performed on those with TLE-1 or CD99 expression.

Results: 7/98 cases (7%) of carcinomas showed TLE-1 expression, including one each of prostate ADCA, esophageal ADCA, BCC, ACC, endometrial ADCA, ovarian serous carcinoma, and SCC. 21/100 cases (21%) of carcinomas showed CD99 expression, including 6 prostate ADCA, 3 esophageal ADCA, 5 SqCC, 2 HCC, 1 each for endometrial ADCA, RCC, UCC, NEC, and MEC. An esophageal ADCA was positive for both TLE-1 and CD99. None of the carcinomas with positive TLE-1(n=7) or CD99 (n=21) by IHC showed SS18 gene rearrangement by FISH.

Conclusions: TLE-1 and CD99 expression were identified in 7% and 21% of carcinomas, respectively. This is a potential pitfall in the IHC interpretation for diagnosis of synovial sarcoma. SS18 gene rearrangement by FISH is helpful for diagnostically challenging cases, either for confirmation or exclusion of synovial sarcoma.

100 Spindle Cell Lipoma Arising at Atypical Locations: A Clinicopathologic Review of 56 Cases

Pingchuan Zhang, Nasir Ud Din, Andrew L Folpe, Karen Fritchie. Mayo Clinic, Rochester, MN; Aga Khan University Hospital, Karachi, Pakistan.

Background: Spindle cell lipomas (SCL) are benign lipomatous tumors that classically arise in the posterior neck/upper back/shoulders of older male patients and are composed of mature adipose tissue, ropey collagen and bland spindle cells. Less commonly, this entity may occur in the trunk, groin or extremities raising concern for atypical lipomatous tumor (ALT).

Design: 439 cases of SCL were identified from our institutional and consultation archives from 1990 to 2015. Cases arising in head, neck, upper back and proximal upper extremities were excluded. All available H&E slides were reviewed for each case, and the diagnoses were confirmed. Tumors with features compatible with extra-mammary myofibroblastoma were excluded. Morphologic patterns, including conventional, myxoid, pseudoangiomatoid, low-fat/fat-free and mature adipose-predominant, were catalogued for each case. CD34 and desmin immunohistochemistry, fluorescence in situ hybridization (FISH) studies for *CPM* amplification and clinical variables were analyzed when available.

Results: 56 cases of SCL arising at atypical locations were identified from 31 males and 25 females (age range: 27 to 79 years, median 53 years). The tumor sites included: distal arm (13), hand (1), finger (8), leg (22), foot (2), toe (1), perineum (3), buttock/perirectal (3), inguinal (2) and flank (1). Tumor sizes were available in 22 cases and ranged from 1.2 to 13 cm (median 4.6 cm). Microscopically, the conventional pattern was identified in nearly all tumors (54 cases, 96%), while the remaining patterns were present less frequently (mature adipose-predominant, 26 cases (46%); myxoid, 8 cases (14%); low-fat/fat-free, 5 cases (9%); pseudoangiomatoid, 1 case (2%)). CD34 was positive in all cases tested (11/11), while desmin was negative when performed (0/7). No cases showed *CPM* amplification (0/15). Follow-up was available in 10 patients (6 to 112 months), and no local recurrences have been reported.

Conclusions: SCLs may arise in the trunk, distal upper extremities and lower extremities and exhibit similar morphologic patterns and clinical behavior to those seen at classic locations. While the vast majority of SCLs arising in the head/neck/upper back occur in male patients, there is relatively equal sex distribution in tumors at atypical sites. Pathologists should be aware that SCLs may arise at these sites to avoid misclassification as ALT.